Phylogeny of the cestode family Escherbothriidae (Cestoda: Rhinebothriidea) reveals unexpected patterns of association with skate hosts

Authors: Bueno, V. M., Trevisan, B., and Caira, J. N.

Source: Invertebrate Systematics, 38(4)

Published By: CSIRO Publishing

URL: https://doi.org/10.1071/IS23056

RESEARCH PAPER
https://doi.org/10.1071/IS23056

Invertebrate Systematics

Phylogeny of the cestode family Escherbothriidae (Cestoda: Rhinebothriidea) reveals unexpected patterns of association with skate hosts

V. M. Bueno[A,*], B. Trevisan[B] and J. N. Caira[A]

For full list of author affiliations and declarations see end of paper

***Correspondence to:**
V. M. Bueno
Department of Ecology and Evolutionary Biology, University of Connecticut, Unit 3043, 75 N. Eagleville Road, Storrs, CT 006269-3043, USA
Email: veronica.m.bueno@uconn.edu

Handling Editor:
Katrine Worsaae

ABSTRACT

The rhinebothriidean tapeworm family Escherbothriidae has recently been expanded to include the genus *Ivanovcestus*, species of which parasitise arhynchobatid skates. Similarities in morphology and host associations between *Ivanovcestus* and *Semiorbiseptum* – a genus yet to be assigned to one of the families in the order Rhinebothriidea – led us to explore the possibility that *Semiorbiseptum* might also belong in the Escherbothriidae. Morphological similarities with *Scalithrium ivanovae*, *Scalithrium kirchneri* and *Rhinebothrium scobinae*, all of which also parasitise arhynchobatid skates, raised questions regarding the generic placements of these species. In addition, new collections from the skate *Sympterygia brevicaudata* revealed two new species that morphologically resemble species of *Ivanovcestus*. A combination of morphological and molecular data were used to assess the generic placement of the newly discovered species and refine our understanding of the membership of the family Escherbothriidae. Sequence data for the D1–D3 region of the *28S rDNA* gene were generated *de novo* for 14 specimens of 7 rhinebothriidean species and combined with comparable published data to represent all 6 families in the Rhinebothriidea in the analysis. The phylogenetic tree resulting from maximum likelihood analysis strongly supports the inclusion of the genus *Semiorbiseptum* in the family Escherbothriidae. Our work also suggests that the skate-hosted species previously assigned to *Scalithrium* and *Rhinebothrium* are also members of *Semiorbiseptum* and that *Ivanovcestus* is a junior synonym of *Semiorbiseptum*. Six species are transferred to *Semiorbiseptum,* bringing the total number of species in the genus to ten. The diagnosis of *Semiorbiseptum* is amended to accommodate the additional species. A second species in the previously monotypic type genus of the family, *Escherbothrium*, is described. The diagnosis of the Escherbothriidae is amended to include the new and transferred species. This study underscores the importance of integrating morphological and molecular data in bringing resolution to cestode systematics. We believe our findings provide a robust foundation for future research into the evolutionary history and host associations of cestodes within the order Rhinebothriidea and beyond. These also highlight the importance of expanding our understanding of skate-hosted cestodes.

ZooBank: urn:lsid:zoobank.org:pub:8052AFCA-5FBD-4430-95F4-0E5E368DEA3D

Keywords: biodiversity, host relationships, molecular phylogenetics, molecular systematics, molecular taxonomy, morphology, nuclear DNA, Platyhelminthes.

Received: 12 December 2023
Accepted: 17 February 2024
Published: 8 April 2024

Cite this: Bueno VM *et al.* (2024) Phylogeny of the cestode family Escherbothriidae (Cestoda: Rhinebothriidea) reveals unexpected patterns of association with skate hosts. *Invertebrate Systematics* **38**, IS23056. doi:10.1071/IS23056

Introduction

The complex evolutionary history of the orders of cestodes hosted by elasmobranchs has intrigued parasitologists and evolutionary biologists for generations. Recent advancements in molecular techniques and taxonomic methodologies have provided new insights into the phylogeny and classification of several of these groups. Among the most notable are the Rhinebothriidea, with relatively recent work resulting in the establishment of the order (Healy *et al.* 2009), circumscription of a phylogenetically informed family-level

classification (Ruhnke *et al.* 2015) and the erection of two additional families (Trevisan *et al.* 2017; Herzog *et al.* 2023).

Escherbothriidae Ruhnke, Caira & Cox, 2015 remains one of the most enigmatic families within Rhinebothriidea. At the time the family was erected, only the monotypic type genus *Escherbothrium* Berman & Brooks, 1994 and an undescribed genus referred to by Ruhnke *et al.* (2015) as new genus 3, which has subsequently been formally established as *Stillabothrium* Healy & Reyda, 2016 (see Reyda *et al.* 2016), were included. The single species of the type genus, *Escherbothrium molinae* Berman & Brooks, 1994, was described from the Chilean round stingray, *Urotrygon chilensis* (Günther), by Berman and Brooks (1994) off the Pacific coast of Costa Rica. Since that time, a second undescribed species, referred to as *Escherbothrium* sp., was included in the molecular phylogenetic analysis of Ruhnke *et al.* (2015). This undescribed species was collected from Roger's round stingray, *Urotrygon rogersi* (Jordan & Sparks), also off the Pacific coast of Costa Rica. With 13 valid species (Ruhnke *et al.* 2022) and many more species remaining to be described (Herzog *et al.* 2021), *Stillabothrium* is a considerably more diverse genus than originally anticipated. Furthermore, the members parasitise a much wider array of elasmobranchs, having been reported from numerous species in the orders Myliobatiformes (i.e. stingrays) and Rhinopristiformes (i.e. guitarfish and relatives). Despite differences in host associations, members of the two genera share possession of bothridia with large facial loculi of various shapes and arrangements (Ruhnke *et al.* 2015). However, recent erection of the genus *Ivanovcestus* Franzese, Montes, Shimabukuro & Arredondo, 2024 by Franzese *et al.* (2024) has added new dimensions to the family. The bothridia of all three species of *Ivanovcestus* bear numerous horizontal loculi and two pairs of posterior loculi. Furthermore, all three species of *Ivanovcestus* parasitise elasmobranchs of the order Rajiformes (i.e. skates) and members of the genus *Sympterygia* Müller & Henle in particular.

Similarities in morphology and host associations between *Ivanovcestus* and *Semiorbiseptum* Franzese & Ivanov, 2020, a genus of rhinebothriideans that has yet to be formally assigned to a family partly because it has not yet been included in a molecular phylogenetic analysis, led us to explore the possibility that *Semiorbiseptum* might also belong in the Escherbothriidae. Morphological similarities also raised questions about the generic placements of *Scalithrium ivanovae* Franzese, 2021, *Scalithrium kirchneri* Franzese & Ivanov, 2021, and *Rhinebothrium scobinae* Euzet & Carvajal, 1973, all of which also parasitise skates. In addition, new collections from the skate *Sympterygia brevicaudata* (Cope) revealed two new species that morphologically resemble species of *Ivanovcestus*. To explore the affinities of these taxa further, we focused on generating new morphological and molecular data for as many of these skate-hosted species as possible.

Our results were somewhat unexpected. Beyond the description of the two new species, our work suggests that all skate-hosted rhinebothriideans that lack a myzorhynchus (and therefore do not belong in the Echeneibothriidae de Beauchamp, 1905) are members of the genus *Semiorbiseptum*. Results further suggest that *Ivanovcestus* is a junior synonym of the latter genus. The diagnosis of *Semiorbiseptum* is amended to accommodate the new species. We also took this opportunity to describe the species referred to as *Escherbothrium* sp. by Ruhnke *et al.* (2015). The diagnosis of the Escherbothriidae is amended to include the new species.

Materials and methods

Collection of cestodes

Each elasmobranch specimen was assigned a unique combination of collection code and collection number. Additional information on each host specimen can be found in the Global Cestode Database (J. N. Caira, K. Jensen and E. Barbeau, see www.tapewormdb.uconn.edu, accessed 28 October 2023) by searching the unique collection code and number (e.g. CHL-117). Elasmobranch specimens examined included the following: nine specimens of *Sympterygia brevicaudata* consisting of eight males 41.2–46.5 cm in disc width (DW) (CHL-94, CHL-106, CHL-116, CHL-117, CHL-118, CHL-120, CHL-122, CHL-123) and one female 43.7 cm in DW (CHL-115); twelve specimens of *Psammobatis scobina* (Philippe) consisting of nine males 25–28.8 cm in DW (CHL-91, CHL-92, CHL-93, CHL-108, CHL-110, CHL-112, CHL-113, CHL-119, CHL-121) and three females 22.2–24.1 cm in DW (CHL-109, CHL-111, CHL-124). All 21 of these specimens were obtained from local fishermen using a bottom trawl off the coast of Viña del Mar, Chile (32°53′22.9″S, 71°31′32.1″W) in January 2014 by F. Concha and V. Bueno. Two specimens of *Urotrygon chilensis* were also examined, including one male 17 cm in DW (MX-8) and one female 18.5 cm in DW (MX-9), obtained from local artisanal fishermen using a bottom trawl off the coast of Salina Cruz, Oaxaca, Mexico (16°09′29.5″N 95°11′26.5″W) in January 2016 by A. Gusmán. In addition, we examined four specimens of *Urotrygon rogersi* consisting of one male 24.5 cm in DW (CRP-45) and three females 24.5–31 cm in DW (CRP-48, CRP-51 and CRP-52), collected using a bottom trawl off the Pacific coast of Costa Rica (10°42′29.5″N, 85°40′9.2″W) in March 2011 by J. Cielocha, and three specimens of *U. rogersi* consisting of one male 21.5 cm in DW (MX-50) and two females 24.7–28.3 cm in DW (MX-46 and MX-48), collected from local artisanal fishermen using a bottom trawl off the coast of Puerto Escondido, Oaxaca, Mexico (15°51′36.7″N, 97°3′44.0″W) in November 2016 by F. Concha and A. Gusmán. Eight specimens of *Psammobatis normani* McEachran were also examined; these consisted of six females 24.6–30.2 cm in DW (FA-49, FA-67, FA-82, FA-85, FA-86,

FA-90) and two males 28–30.2 cm in DW (FA-79, FA-80) collected using a bottom trawl onboard the Research Cruise ZDLT off the coast of the Falkland Islands (50°22′27.0″S, 58°01′40.2″W) in July 2017 by F. Concha. We also examined one female specimen of *Sympterygia bonapartii* Müller & Henle (SC09-7) collected off the coast of Balneário Arroio do Silva, Santa Catarina, Brazil in August 2009 (29°02′40.2″S, 49°17′31.5″W) and four female specimens of *Rioraja agassizii* (Müller & Henle) (RJ08-14, SC09-13, SP11-11, SP19-30), all of unknown DW, collected off the coast of Macaé, State of Rio de Janeiro (22°38′37.1″S, 41°54′6.9″W), Balneário Arroio do Silva, State of Santa Catarina (29°02′40.2″S, 49°17′31.5″W) and Ubatuba, State of São Paulo (23°27′42.3″S, 45°00′50.2″W) in Brazil in September 2008, August 2009, December 2011 and August 2019 respectively by F. Marques. In an effort to obtain additional material of *Scalithrium*, one female specimen of *Acroteriobatus annulatus* (Smith) 24 cm in DW (AF-182) collected using a bottom trawl on the *FV Africana* off Cape St Francis, South Africa (34°10′00.0″S, 24°54′00.0″E) in May 2010 by J. N. Caira and K. Jensen was examined.

A small sample of liver tissue was taken from each elasmobranch specimen and preserved in 95% ethanol for molecular verification of host identity. The spiral intestine of each specimen was removed via a ventral incision in the body cavity and opened with a longitudinal incision to ensure proper fixation. Spiral intestines were fixed in either seawater-buffered formalin (9:1) or 95% ethanol. In some cases, a subset of cestodes was removed from the spiral intestine in the field, sorted under a dissecting microscope and preserved in seawater-buffered formalin (9:1) or 95% ethanol. After ~1 week, formalin-fixed spiral intestines and cestodes were transferred to 70% ethanol for storage. Samples fixed in 95% ethanol were stored at −20°C.

Additional material examined

We examined the holotype (USNM number 1379291) and seven voucher specimens of *Escherbothrium molinae* (LRP numbers 11050–11056) from *Urotrygon chilensis* collected off Costa de Pajaros, Costa Rica for comparative purposes. In addition, photographs of the holotype of *Ivanovcestus chilensis* (Euzet & Carvajal, 1973) Franzese, Montes, Shimabukuro & Arredondo, 2024 (MNHNC number 20005), the holotype of *Ivanovcestus leiblei* (Euzet & Carvajal, 1973) Franzese, Montes, Shimabukuro & Arredondo, 2024 (MNHNC number 20006), and the holotype of *Rhinebothrium scobinae* (MNHNC number 20007) were also examined.

Morphological methods

Cestodes prepared for light microscopy were hydrated in a graded ethanol series, stained for 30–40 min in a working solution of Delafield's hematoxylin (1:9 mixture of hematoxylin:distilled water), differentiated in tap water, destained in acidic 70% ethanol, neutralised in basic 70% ethanol, dehydrated in a graded ethanol series, cleared in methyl salicylate, mounted in Canada balsam on glass slides under glass coverslips, and left to dry in an oven set to 55°C for ~1 week. Measurements and images were taken using a SPOT Diagnostic Instrument Digital Camera System and SPOT software (ver. 4.6, SPOT Imaging Solutions, Sterling Heights, MI, USA) on a Zeiss Axioskop 2 Plus compound microscope equipped with a Nomarski Differential Interference Contrast (DIC) system (Zeiss, Thornwood, NY, USA). Measurements are given as the range in micrometres unless stated otherwise. In instances in which more than five measurements were taken, the range is followed by the mean, standard deviation, number of specimens measured (*N*) and total number of measurements (*n*) in parentheses when more than one measurement was made per worm. Shape terminology follows Clopton (2004).

Specimens were prepared for scanning electron microscopy (SEM) by removing the strobila and preparing it as a whole mount as described above to serve as a voucher. Scoleces were hydrated in a graded ethanol series, transferred to a 1% solution of osmium tetroxide overnight, dehydrated in a graded ethanol series, placed in hexamethyldisilazane in a fume hood for 30 min and allowed to air dry. Specimens were mounted on double-sided PELCO carbon tabs (Ted Pella Inc., Redding, CA, USA) on aluminium stubs, sputter coated with 20 nm of gold–palladium and examined with an FEI Nova NanoSEM 450 field emission SEM (FEI, Hillsboro, OR, USA) at the Bioscience Electron Microscopy Laboratory, University of Connecticut (Storrs, CT, USA). Microthrix terminology follows Chervy (2009).

Museum abbreviations used include the following: MZUCR, Museo de Zoología, Centro de Investigación de Biodiversidad y Ecología Tropical; CIBET, University of Costa Rica, San José, Costa Rica; CNHE, Colección Nacional de Helmintos, Instituto de Biología, Universidad Autónoma de México, Mexico City, Mexico; LRP, Lawrence R. Penner Parasitology Collection, University of Connecticut, Storrs, CT, USA; MNHNC, Museo Nacional de Historia Natural Chile, Invertebrate Zoology, Santiago, Chile; MZUSP, Museu de Zoologia da Universidade de São Paulo, São Paulo, Brazil; NHMUK, The Natural History Museum, London, UK; USNM, National Museum of Natural History, Smithsonian Institution, Department of Invertebrate Zoology, Washington, DC, USA.

Molecular methods

Sequence data for the D1–D3 region of the *28S rDNA* gene were generated *de novo* for 14 specimens of seven rhinebothriidean species. In most cases, the scolex and terminal portion of the strobila were prepared as whole mounts as described above to serve as hologenophores (*sensu* Pleijel *et al.* 2008) of the specimen sequenced. Eleven hologenophores were deposited in LRP; the remaining specimens are represented by images and a paragenophore that have

also been deposited in LRP. GenBank accession numbers for all 14 sequences are provided on the phylogenetic tree (Fig. 1). Detailed information about each voucher specimen can be obtained from the LRP database (see https://lrpennerdb.uconn.edu/) by searching the accession number.

The specimens sequenced included two detached proglottids of *Escherbothrium molinae* from *U. chilensis* (DA-29, DA-30, image vouchers LRP numbers 11062, 11063 respectively). In addition, one complete worm collected from the same host individual as the specimens sequenced was also

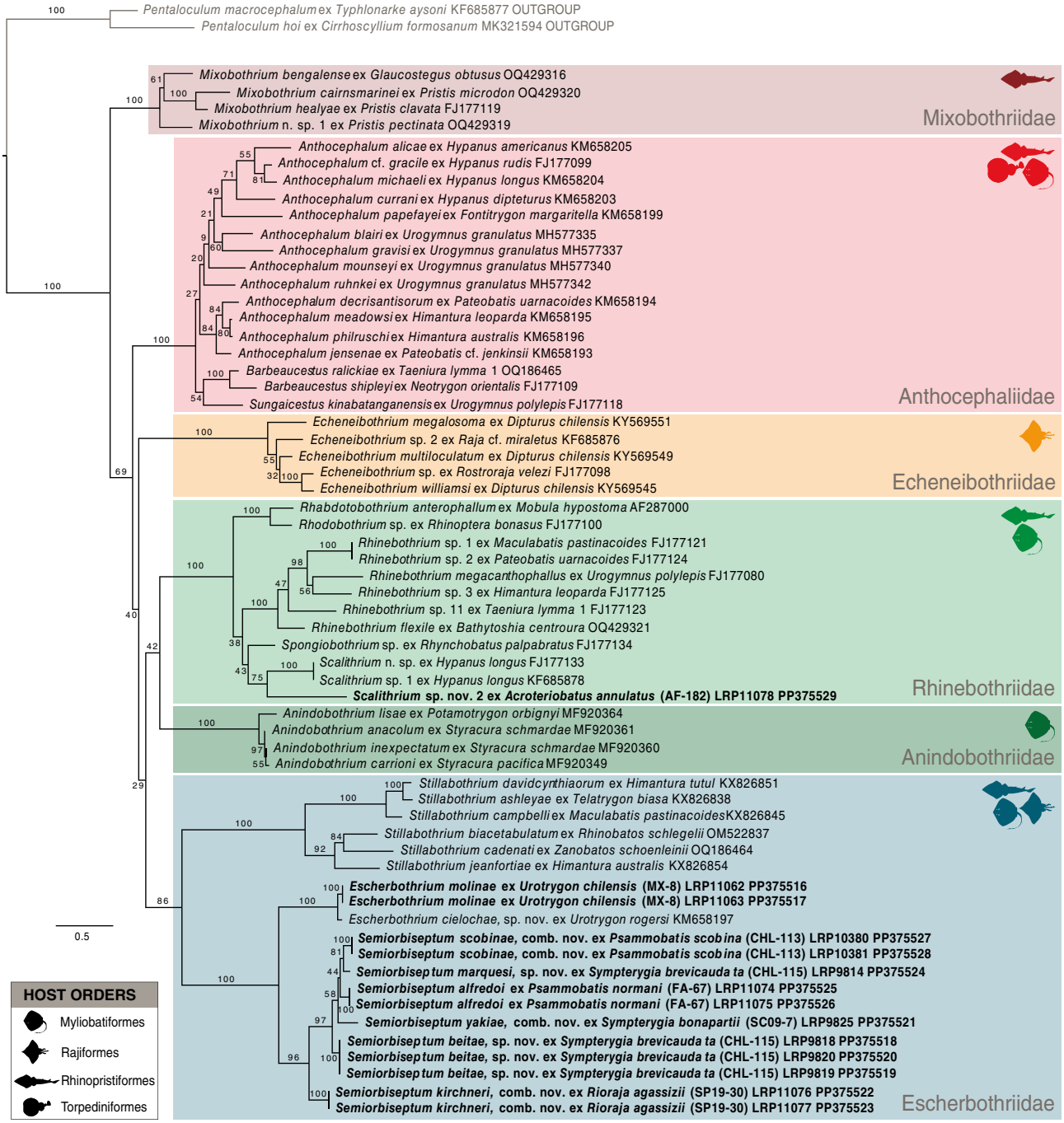

Fig. 1. Phylogenetic relationships within the Rhinebothriidea based on maximum likelihood analysis of the D1–D3 region of the *28S rDNA* gene (1289 bp). Taxon labels include cestode species followed by host species and GenBank accession numbers. Sequences generated *de novo* are marked in bold. Taxon labels of newly generated sequences include the cestode species followed by host species and host specimen code in parentheses, Lawrence R. Penner Parasitological Collection (LRP) hologenophore accession number and GenBank accession number. Support values on nodes are the result of 200 replicates of non-parametric bootstrap analysis. Scale bar indicates number of substitutions per site.

deposited to serve as a paragenophore (LRP number 11060). We also sequenced two specimens of *Rhinebothrium scobinae* from *P. scobina* (BU064, BU065, hologenophores LRP numbers 10380, 10381 respectively), two specimens of *Semiorbiseptum alfredoi* Franzese & Ivanov, 2020 from *P. normani* (DA-6, KW1030, hologenophores LRP numbers 11074, 11075 respectively), one specimen of a new species of *Semiorbiseptum* from *S. brevicaudata* (VB123, hologenophore LRP number 9814), three specimens of a second new species of *Semiorbiseptum* also from *S. brevicaudata* (VB121, VB122, VB126, hologenophores LRP numbers 9818–9820 respectively), one specimen of *Ivanovcestus yakiae* Franzese, Montes, Shimabukuro & Arredondo, 2024 from *S. bonapartii* (VB220, voucher image LRP number 9825), two specimens of *Scalithrium kirchneri* from *R. agassizii* (DA-3, DA-4, hologenophores LRP numbers 11076, 11077 respectively) and one specimen of an undescribed species referred to as *Scalithrium*, sp. nov. 2 from *A. annulatus* (KW277, hologenophore LRP number 11078).

The middle portion of each specimen was removed and allowed to air dry for 5 min at room temperature to be used for DNA extraction. Total genomic DNA (gDNA) was extracted using the MasterPure DNA Purification Kit (Epicentre Technologies, Madison, WI, USA) following the manufacturer's instructions for small tissue samples. DNA was quantified using a micro-volume spectrophotometer NanoDrop 2000 (ThermoFisher Scientific, Waltham, MA, USA). Polymerase chain reaction (PCR) was used to amplify the target region. Double-stranded amplifications were generated using one of two protocols. The first protocol used a total reaction volume of 10 µL containing 1–3 µL of DNA template, 5.0 µL of GoTaq Green Master Mix (PROMEGA, Fitchburg, WI, USA), 0.1 µL of each 10-µM primer and 1.8–3.8 µL of double distilled water. The second protocol used a total reaction volume of 12.5 µL containing 1–2 µL of DNA template, 0.1 µL of Ex Taq, 1.25 µL of 10× ex Taq buffer, 1.0 µL of 2.5 mM dNTPs (Takara Bio USA, San Jose, CA, USA), 0.5 µL of each 10-µM primer and 7.15–8.15 µL of double distilled water. Amplification was undertaken using the primer pair LSU-5 (5′ TAGGTCGACCCGCTGAAYTTA 3′) (Littlewood *et al.* 2000) and LSU-1500R (5′ GCTATCCTGG AGGGAAACTTCG 3′) (Tkach *et al.* 2003). Sequencing was undertaken using the primer pair LSU-55F (5′ AACCAGGA TTCCCCTAGTAACGGC 3′) (Bueno and Caira 2017) or ZX-1 (5′ ACCCGCTGAATTTAAGCATAT 3′) (Van der Auwera *et al.* 1994) and LSU-1200R (5′ GCATAGTTCACCATCTTTCGG 3′) (Littlewood *et al.* 2000). PCR cycling conditions included an initial denaturation of 1 min at 94°C, followed by 39 cycles of denaturation for 30 s at 94°C, annealing for 1 min at 56°C or 59°C, extension for 1 min at 72°C and a final extension of 5 min at 72°C. PCR product cleanup was performed by adding 1 µL of diluted (1:5) ExoSAP-IT (Affymetrix, Inc., Santa Clara, CA, USA) to every 8 µL of PCR product. Cleanup conditions included 30 min at 37°C, followed by 15 min at 80°C and a cool-down step of 10 min at 20°C. The cycle sequencing reaction protocol included an initial denaturation step of 2 min at 96°C and 40 cycles of a denaturation step of 30 s at 96°C, an annealing step of 30 s at 50°C and an extension step of 4 min at 60°C. Cycle sequencing products were cleaned with Sephadex beads (Sigma–Aldrich, St Louis, MO, USA). Sequencing of both strands was carried out on an ABI PRISM 3100 Genetic Analyser using ABI Big Dye dideoxy terminators (ver. 3.1, Applied Biosystems, Foster City, CA, USA) and the sequencing primers listed above. Contigs were assembled and sequences edited using Geneious Prime 2022 (ver. 2022.0.1, see www.geneious.com).

Sequence data for the D1–D3 region of the *28S rDNA* gene of two specimens of *Rhinebothrium scobinae* were extracted from the complete ribosomal DNA (rDNA) assembly obtained using the genome skimming method described in Trevisan *et al.* (2019). Complete ribosomal DNA sequences were assembled by baiting and iterative mapping using MIRA (ver. 4.0.2, see https://mira-assembler.sourceforge.net/docs/; Chevreux *et al.* 1999) and a modified version of MITOBIM.PL (ver. 1.6, see https://github.com/chrishah/MITObim; Hahn *et al.* 2013), following Machado *et al.* (2016, see their appendix S2) and Trevisan *et al.* (2019, 2021). Sequence data for *Scalithrium*, sp. nov. 2 were assembled by Hannah Ralicki and Elizabeth Jockusch using MITObim (ver. 1.9.1, see https://github.com/chrishah/MITObim; Hahn *et al.* 2013) from Next Generation Sequencing Illumina short reads generated for a related project.

Alignment and phylogenetic analyses

Sequence data generated *de novo* were combined with comparable data available from GenBank (Table 1) to represent all families currently assigned to the Rhinebothriidea in the analysis. These taxa consisted of four species of anindobothriids, 16 species of anthocephaliids, 5 species of echeneibothriids, 7 species of escherbothriids, 4 species of mixobothriids and 11 species of rhinebothriids. Sequence data for two species of *Pentaloculum* Alexander, 1963 were also obtained from GenBank to serve as outgroup taxa.

Sequences were aligned and trimmed using the MAFFT Multiple Alignment (ver. 1.5.0, see https://mafft.cbrc.jp/alignment/server/; Katoh and Standley 2013; Katoh *et al.* 2019) plugin in Geneious Prime 2022 (ver. 2022.0.1) using default parameter settings. The final alignment consisted of 63 taxa and was 1289 bp long. Maximum likelihood (ML) phylogenetic analysis was performed on the cluster in the Bioinformatics facility of the Institute of Systems Genomics at the University of Connecticut using IQ-TREE (ver. 2.2.2.7, see http://www.iqtree.org/; Minh *et al.* 2020). GTR + F + I + G4 was selected as the best-ranked model of molecular evolution according to the Bayesian Information Criterion (BIC) as implemented in ModelFinder (Kalyaanamoorthy *et al.* 2017) in IQ-TREE. This was followed by ML tree reconstruction and generation of 200 non-parametric bootstrap replicates using the command *iqtree -s datamatrix.nex*

Table 1. Information on the source of the sequence data obtained from GenBank for specimens included in the phylogenetic analysis.

Ingroup or outgroup Genus	Species	Family	Host species	Unique host code	Voucher Accession numbers	GenBank Accession numbers	Source
Ingroup							
Anindobothrium	*carrioni*	Anindobothriidae	*Styracura pacifica*	PN15-25	MZUSP number 7788	MF920349	Trevisan *et al.* (2017)
Anindobothrium	*lisae*	Anindobothriidae	*Potamotrygon orbignyi*	VZ11-29	MZUSP number 7784	MF920364	Trevisan *et al.* (2017)
Anindobothrum	*inexpectatum*	Anindobothriidae	*Styracura schmardae*	BE-9	MZUSP number 7774	MF920360	Trevisan *et al.* (2017)
Anindobothrum	*anacolum*	Anindobothriidae	*Potamotrygon yepezi*	VZ11-1	MZUSP number 7781	MF920361	Trevisan *et al.* (2017)
Anthocephalum	*alicae*	Anthocephaliidae	*Hypanus americanus*[A]	TM-19	LRP number 8506	KM658205	Ruhnke *et al.* (2015)
Anthocephalum	*blairi*	Anthocephaliidae	*Urogymnus granulatus*	SO-9	LRP number 9849	MH577335	Herzog and Jensen (2018)
Anthocephalum	cf. *gracile*	Anthocephaliidae	*Hypanus rudis*[A]	SE-122	LRP number 4219	FJ177099	Healy *et al.* (2009)
Anthocephalum	*currani*	Anthocephaliidae	*Hypanus dipterura*[A]	BJ-119	LRP number 8510	KM658203	Ruhnke *et al.* (2015)
Anthocephalum	*decrisantisorum*	Anthocephaliidae	*Pateobatis uarnacoides*[A]	BO-91	LRP number 8511	KM658194	Ruhnke *et al.* (2015)
Anthocephalum	*gravisi*	Anthocephaliidae	*Urogymnus granulatus*	SO-19	LRP number 9862	MH577337	Herzog and Jensen (2018)
Anthocephalum	*jensenae*	Anthocephaliidae	*Pateobatis* cf. *jenkinsii*[A]	NT-118	LRP number 8513	KM658193	Ruhnke *et al.* (2015)
Anthocephalum	*meadowsi*	Anthocephaliidae	*Himantura leoparda*	NT-32	LRP number 8514	KM658195	Ruhnke *et al.* (2015)
Anthocephalum	*michaeli*	Anthocephaliidae	*Hypanus longus*[A]	BJ-423	LRP number 8515	KM658204	Ruhnke *et al.* (2015)
Anthocephalum	*mounseyi*	Anthocephaliidae	*Urogymnus granulatus*	SO-9	LRP number 9888	MH577340	Herzog and Jensen (2018)
Anthocephalum	*papefayei*	Anthocephaliidae	*Fontitrygon margaritella*[A]	SE-225	LRP number 8517	KM658199	Ruhnke *et al.* (2015)
Anthocephalum	*philruschi*	Anthocephaliidae	*Himantura australis*[A]	CM03-24	LRP number 8518	KM658196	Ruhnke *et al.* (2015)
Anthocephalum	*ruhnkei*	Anthocephaliidae	*Urogymnus granulatus*	SO-9	LRP number 9893	MH577342	Herzog and Jensen (2018)
Barbeaucestus	*ralickiae*	Anthocephaliidae	*Taeniura lymma* 1	BO-131	LRP number 9832	OQ186465	Bueno and Caira (2023)
Barbeaucestus	*shipleyi*	Anthocephaliidae	*Neotrygon orientalis*[A]	BO-336	LRP number 3894	FJ177109	Healy *et al.* (2009)

(*Continued on next page*)

Table 1. (*Continued*)

Ingroup or outgroup Genus	Species	Family	Host species	Unique host code	Voucher Accession numbers	GenBank Accession numbers	Source
Sungaicestus	*kinabatanganensis*	Anthocephaliidae	*Urogymnus polylepis*[A]	BO-108	LRP number 3900	FJ177118	Healy *et al.* (2009)
Echeneibothrium	*megalosoma*	Echeneibothriidae	*Dipturus chilensis*	CHL-51	LRP number 9228	KY569551	Bueno and Caira (2017)
Echeneibothrium	*multiloculatum*	Echeneibothriidae	*Dipturus chilensis*	CHL-67	LRP number 9230	KY569549	Bueno and Caira (2017)
Echeneibothrium	sp.	Echeneibothriidae	*Rostroraja velezi*[A]	BJ 243	LRP number 4217	FJ177098	Healy *et al.* (2009)
Echeneibothrium	sp. 2	Echeneibothriidae	*Raja* cf. *miraletus*[A]	SE-188	LRP number 8312	KF685876	Caira *et al.* (2014)
Echeneibothrium	*williamsi*	Echeneibothriidae	*Dipturus chilensis*	CHL-73	LRP number 9234	KY569545	Bueno and Caira (2017)
Escherbothrium	*cielochae*, sp. nov.	Escherbothriidae	*Urotrygon rogersi*[A]	CRP-50	LRP number 8519	KM658197	Ruhnke *et al.* (2015)
Stillabothrium	*ashleyae*	Escherbothriidae	*Telatrygon biasa*[A]	KA-182	LRP number 8992	KX826838	Reyda *et al.* (2016)
Stillabothrium	*biacetabulatum*	Escherbothriidae	*Rhinobatos schlegelii*	TW-16	LRP number 10812	OM522837	Ruhnke *et al.* (2022)
Stillabothrium	*cadenati*	Escherbothriidae	*Zanobatos schoenleinii*	SE-201	LRP number 9831	OQ186464	Bueno and Caira (2023)
Stillabothrium	*campbelli*	Escherbothriidae	*Maculabatis pastinacoides*[A]	BO-100	LRP number 9149	KX826845	Reyda *et al.* (2016)
Stillabothrium	*davidcynthiaorum*	Escherbothriidae	*Himantura tutul*[A]	BO-47	LRP number 8989	KX826851	Reyda *et al.* (2016)
Stillabothrium	*jeanfortiae*	Escherbothriidae	*Himantura australis*	CM03-3	LRP number 8999	KX826854	Reyda *et al.* (2016)
Mixobothrium	*bengalense*	Mixobothriidae	*Glaucostegus obtusus*	IN-8	LRP number 10970	OQ429316	Herzog *et al.* (2023)
Mixobothrium	*cairnsmarinei*	Mixobothriidae	*Pristis pristis*	CM03-1	LRP number 10963	OQ429320	Herzog *et al.* (2023)
Mixobothrium	*healyae*	Mixobothriidae	*Pristis clavata*	AU-36	LRP number 4220	FJ177119	Healy *et al.* (2009)
Mixobothrium	sp. nov. 1	Mixobothriidae	*Pristis pectinata*	FWH-1800008	LRP number 10973	OQ429319	Herzog *et al.* (2023)
Rhabdotobothrium	*anterophallum*	Rhinebothriidae	*Mobula hypostoma*	SAB-6	NHMUK number 2001.1.31.3-4	AF287000	Olson *et al.* (2001)

(*Continued on next page*)

Table 1. (*Continued*)

Ingroup or outgroup Genus	Species	Family	Host species	Unique host code	Voucher Accession numbers	GenBank Accession numbers	Source
Rhinebothrium	*flexile*	Rhinebothriidae	*Bathytoshia centroura*	SAB-7	LRP number 10974	OQ429321	Herzog *et al.* (2023)
Rhinebothrium	*megacanthophallus*	Rhinebothriidae	*Urogymnus polylepis*[A]	BO-108	LRP number 3901	FJ177080	Healy *et al.* (2009)
Rhinebothrium	sp. 1	Rhinebothriidae	*Maculabatis pastinacoides*	BO-76	LRP number 3903	FJ177121	Healy *et al.* (2009)
Rhinebothrium	sp. 11	Rhinebothriidae	*Taeniura lymma* 1[B]	BO-131	LRP number 3923	FJ177123	Healy *et al.* (2009)
Rhinebothrium	sp. 2	Rhinebothriidae	*Pateobatis uarnacoides*	BO-91	LRP number 3907	FJ177124	Healy *et al.* (2009)
Rhinebothrium	sp. 3	Rhinebothriidae	*Himantura leoparda*[A]	NT-117	LRP number 3908	FJ177125	Healy *et al.* (2009)
Rhodobothrium	sp.	Rhinebothriidae	*Rhinoptera bonasus*	BNC-22	LRP number 4216	FJ177100	Healy *et al.* (2009)
Scalithrium	sp. nov.	Rhinebothriidae	*Hypanus longus*[A]	BJ-423	LRP number 3895	FJ177133	Healy *et al.* (2009)
Scalithrium	sp. 1	Rhinebothriidae	*Hypanus longus*[A]	BJ-423	LRP number 8333	KF685878	Caira *et al.* (2014)
Spongiobothrium	sp.	Rhinebothriidae	*Rhynchobatus palpebratus*[A]	NT-66	LRP number 3919	FJ177134	Healy *et al.* (2009)
Outgroup							
Pentaloculum	*hoi*	NA	*Cirrhoscyllium formosanum*	TW-159	LRP number 9952	MK321594	Eudy *et al.* (2019)
Pentaloculum	*macrocephalum*	NA	*Typhlonarke aysoni*[A]	CR-136	LRP number 8347	KF685877	Caira *et al.* (2014)

[A]Names updated as per Last *et al.* (2016).
[B]Name updated as per Naylor *et al.* (2012).

-m MFP -b 200. Following Hillis and Bull (1993), nodes with bootstrap values of ≥70% were considered to be strongly supported.

Results

Phylogenetic analysis

The tree resulting from our molecular phylogenetic analysis is presented in Fig. 1. The topology indicates that all skate-hosted rhinebothriideans, apart from the Echeneibothriidae, belong to a well-supported clade within the Escherbothriidae. This clade includes specimens currently referred to as *Rhinebothrium scobinae*, *Scalithrium kirchneri*, *Semiorbiseptum alfredoi* and the type of its genus, *Ivanovcestus yakiae*. Given that *R. scobinae* groups well away from the other species of *Rhinebothrium* and *S. kirchneri* is similarly distant from the other species of *Scalithrium*, neither name is appropriate for this clade and therefore both of these species require new generic assignments. The fact that both *S. alfredoi* and *I. yakiae* are nested deeply within the skate-hosted clade indicates that *Semiorbiseptum* and *Ivanovcestus* are synonyms. As the senior name, *Semiorbiseptum* is the appropriate name for this genus, which also includes both of our new species from skates. The names of the terminal taxa in Fig. 1 reflect this synonymy. The topology, which includes both known species of *Escherbothrium*, also provides evidence that *Escherbothrium* is the sister taxon of *Semiorbiseptum*.

The synonymisation of *Ivanovcestus* with *Semiorbiseptum* also results in the transfer of *Ivanovcestus chilensis* and *I. leiblei* to the latter genus as *Semiorbiseptum chilensis* (Euzet & Carvajal, 1973), comb. nov. and *Semiorbiseptum leiblei* (Euzet & Carvajal, 1973), comb. nov. Based on the morphological similarities and host associations with *S. kirchneri*, we also transfer *Scalithrium ivanovae* Franzese, 2021 to the genus as *Semiorbiseptum ivanovae* (Franzese, 2021), comb. nov. The inclusion of the two new species we described brings the total number of valid species of *Semiorbiseptum* to 10.

Taxonomic treatments

Semiorbiseptum scobinae (Euzet & Carvajal, 1973), comb. nov. amended

(Fig. 2, 3.)

The original description of *Semiorbiseptum scobinae* (Euzet & Carvajal, 1973), comb. nov. provided by Euzet and Carvajal (1973) as *Rhinebothrium scobinae*, is amended to include the following information, based on 2 scoleces observed with SEM, 6 newly collected specimens and holotype.

Bothridia with apical sucker; each bothridium divided into 15–17 (16 ± 0.9; 6) loculi by transverse septa; central region with 3 weakly muscular semicircular septa (Fig. 3); posterior region with short, medial longitudinal septum forming 2 tandem pairs of loculi immediately anterior to single terminal loculus; apical sucker 55–59 (57 ± 1.8; 6, 8) long by 82–99 (88 ± 6.6; 6, 8) wide. Proximal surfaces of bothridia (Fig. 2*e*) covered with papilliform filitriches; distal surfaces of apical sucker (Fig. 2*c*) and bothridia (Fig. 2*d*) covered with capilliform filitriches interspersed with acicular filitriches; cephalic peduncle (Fig. 2*f*) covered with capilliform filitriches.

Type and only known host

Psammobatis scobina (Philippi) (Rajiformes: Arhynchobatidae Fowler).

Type locality

Southern coast of Chile.

Additional localities

Viña del Mar, Chile (32°53′22.9″S, 71°31′32.1″W).

Type specimens examined

Holotype (MNHNC number 20007).

Site of infection

Spiral intestine.

Voucher specimens deposited

Six voucher specimens (LRP numbers 11066–11071), two SEM vouchers (LRP numbers 11072–11073). Scoleces prepared for SEM retained with JNC at the University of Connecticut.

Sequence data

GenBank numbers PP375527 (BU064, hologenophore LRP number 10380), PP375528 (BU065, hologenophore LRP number 10381).

Remarks

Our new material that was collected off Viña del Mar, extends the distribution of *S. scobinae* (Euzet & Carvajal, 1973), comb. nov. from southern Chile further north to central Chile. The original description provides detailed line drawings of this species, however, the central region of each bothridium is shown as lacking septa. Examination of newly collected specimens revealed three weakly muscular semicircular septa in the central region of the bothridia. The presence of semicircular septa has previously been reported in the two original species of *Semiorbiseptum* that also parasitise skates in the genus *Psammobatis* (i.e. *Semiorbiseptum mariae* Franzese & Ivanov, 2020 and *S. alfredoi*; see Franzese and Ivanov, 2020). However, unlike the septa in *S. mariae* and *S. alfredoi*, the

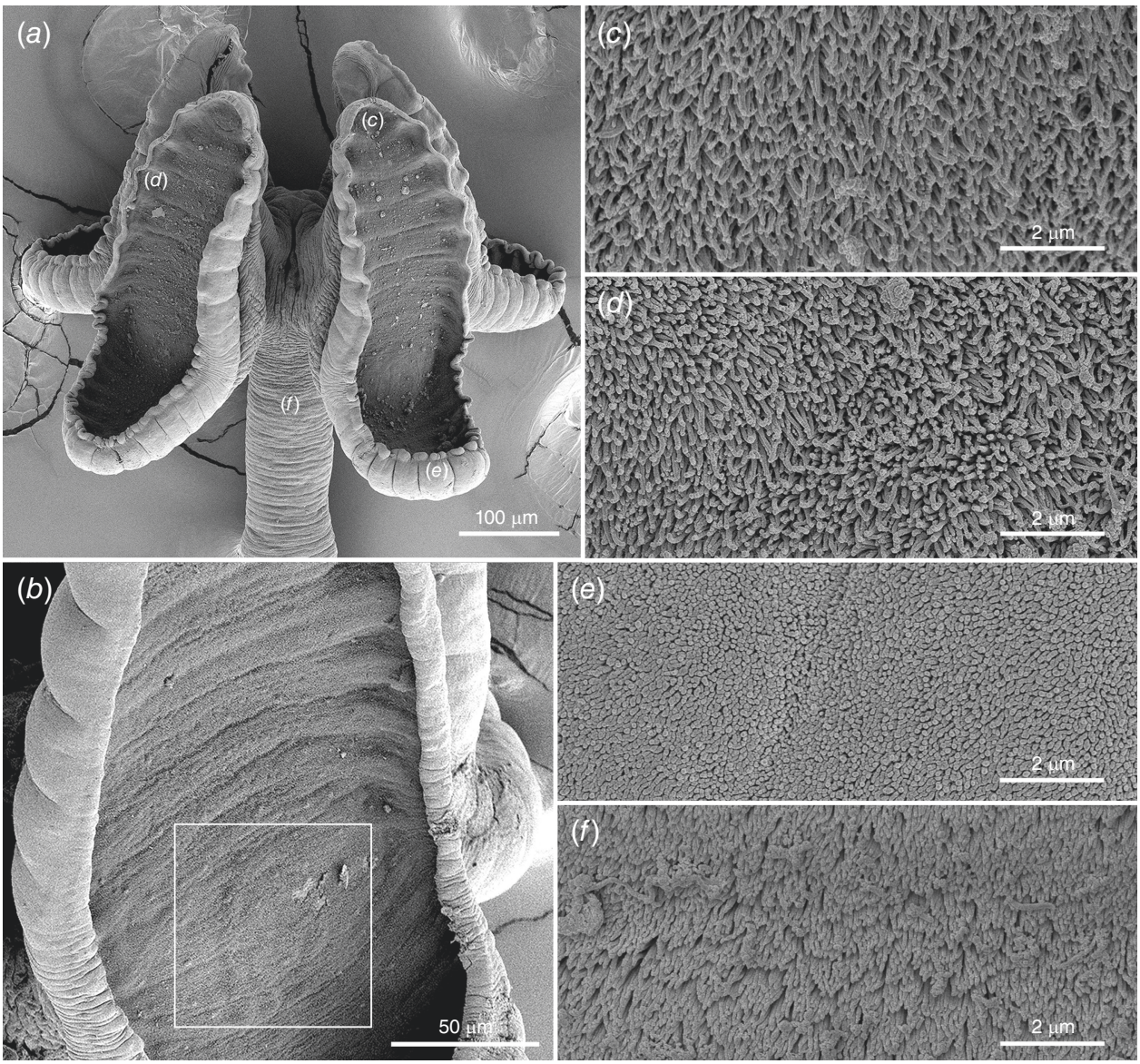

Fig. 2. Scanning electron micrographs of *Semiorbiseptum scobinae* (Euzet & Carvajal, 1973), comb. nov. (*a*) Scolex; the location of details in micrographs *c–f* are indicated in panel *a*. (*b*) Detail of central region of bothridium; square indicates location of inconspicuous semicircular septa. (*c*) Distal surface of apical sucker covered with capilliform filitriches interspersed with acicular filitriches. (*d*) Distal surface of bothridium covered with capilliform filitriches interspersed with acicular filitriches. (*e*) Proximal surface of bothridium covered with papilliform filitriches. (*f*) Cephalic peduncle covered with capilliform filitriches.

semicircular septa in *S. scobinae* (Euzet & Carvajal, 1973), comb. nov. are difficult to observe with SEM (Fig. 2*a*, *b*) and visible under light microscopy only when using DIC (Fig. 3). Interestingly, the complete lack of spinitriches from all surfaces of the bothridia and cephalic peduncle of *S. scobinae* (Euzet & Carvajal, 1973), comb. nov. differs from the pattern observed in the other five members of *Semiorbiseptum* that have been examined with SEM to date; *S. alfredoi*, *S. ivanovae*, *S. kirchneri*, *S. mariae* and *S. yakiae* possess gladiate or coniform spinitriches on at least one of these surfaces.

Semiorbiseptum beitae Bueno, Trevisan & Caira, sp. nov.

(Fig. 4, 5.)

ZooBank: urn:lsid:zoobank.org:act:DCFC78A3-2C22-4174-9D0C-52B65AE29384

Description

Based on 6 complete mature worms, 5 incomplete worms and 2 scoleces observed with SEM.

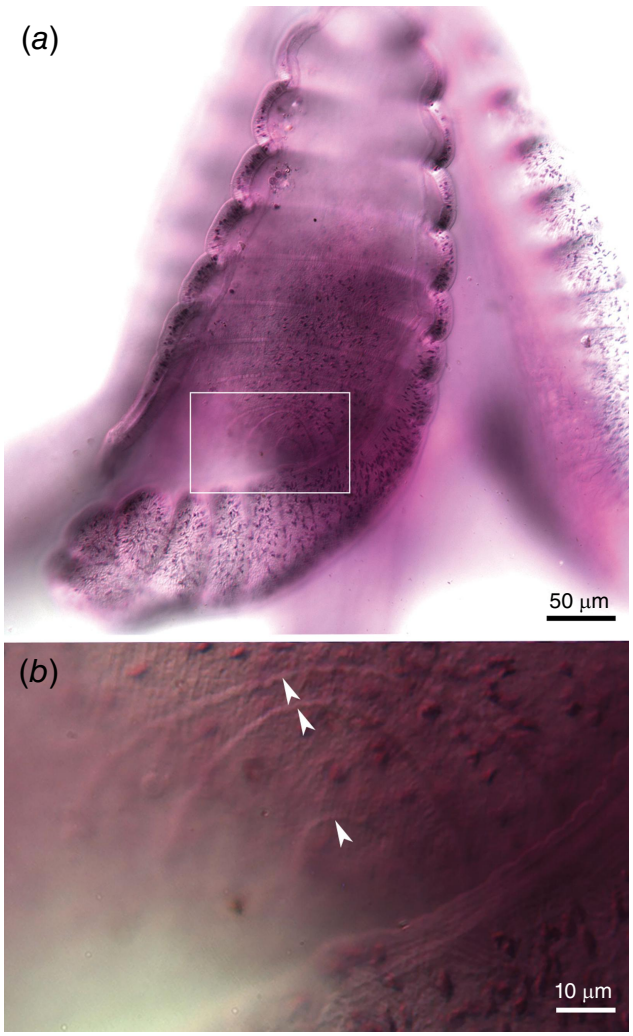

Fig. 3. Photomicrographs of bothridium of *Semiorbiseptum scobinae* (Euzet & Carvajal, 1973), comb. nov. (LRP number 11070). (*a*) Bothridium; rectangle indicates location of micrograph *b*. (*b*) Semicircular septa in the central region of bothridium; arrows indicate each of the three semicircular septa.

Worms euapolytic, 20.8–26 (23 ± 1.9; 6) mm long, greatest width at level of scolex; 260–289 (272 ± 11.3; 6) proglottids per worm. Scolex 1254–2362 (1873 ± 331.1; 11) long by 554–1099 (764 ± 175.8; 11) wide, consisting of 4 stalked bothridia (Fig. 4*b*) and pronounced cephalic peduncle (Fig. 4*a*). Bothridia with apical sucker, 633–810 (712 ± 54.2; 4, 8) long by 134–286 (207 ± 49.7; 8, 11) wide; each bothridium divided by transverse septa into 53–60 (56 ± 2.4; 6; 10) loculi; central region without semicircular septa; posterior region with short, medial longitudinal septum forming 2 tandem pairs of loculi immediately anterior to single terminal loculus; apical sucker 37–56 (47 ± 5; 10, 17) long by 45–59 (52 ± 3.9; 10, 17) wide. Cephalic peduncle 692–1899 (1363 ± 307.9; 11) long by 69–165 (131 ± 27.4; 11) wide at posterior end. Proximal surfaces of bothridia (Fig. 5*c*) covered with acicular filitriches interspersed with small, sparsely distributed gladiate spinitriches; proximal surface of apical sucker (Fig. 5*d*) covered with acicular filitriches; distal surfaces of bothridia (Fig. 5*b*) covered with acicular filitriches; cephalic peduncle (Fig. 5*e*) covered with small, densely distributed gladiate spinitriches.

Proglottids craspedote. Immature proglottids 254–282 (266 ± 11.4; 6) in number, wider than long, becoming longer than wide with maturity. Mature proglottids 5–9 (7 ± 1.4; 6) in number, longer than wide; terminal mature proglottid 772–1110 (982 ± 136.7; 6) long by 233–312 (266 ± 31.3; 6) wide, length:width ratio 2.6–4.5 (4 ± 0.7; 6): 1; gravid proglottids not observed. Genital pores marginal, 42–48% (45 ± 2; 6) of proglottid length from posterior margin in terminal proglottid, irregularly alternating. Testes 27–37 (32 ± 2.9; 11, 30) in number, 28–69 long (41 ± 8.5; 11, 57) by 25–85 (54 ± 16.5; 11, 57) wide, 1 layer deep, arranged in 3–4 irregular columns, extending from anterior margin of proglottid to level of cirrus sac on poral side and level of ovary on aporal side (Fig. 4*c*). Vas deferens highly coiled, extending posteriorly from cirrus sac to level of ovarian bridge. Cirrus sac (Fig. 4*d*) thin-walled, pyriform, slightly tilted posteriorly, containing coiled cirrus, 77–112 (95 ± 14.1; 6) long by 58–74 (65 ± 6.1; 6) wide; cirrus armed with spinitriches. Vagina thick-walled, weakly sinuous, extending from ootype along medial line of proglottid to level of cirrus sac, extending along anterior margin of cirrus sac to open into genital atrium anterior to cirrus; vaginal sphincter lacking; seminal receptacle not observed. Ovary at posterior end of proglottid, with smooth margins, H-shaped in frontal view, tetralobed in cross-section, essentially symmetrical, 239–371 (302 ± 49.1; 6) long by 127–165 (145 ± 15.5; 6) wide. Mehlis' gland posterior to ovarian isthmus. Vitellarium follicular; follicles arranged in 2 lateral bands; each band consisting of 1 dorsal and 1 ventral column of follicles, extending throughout length of proglottid, interrupted ventrally by terminal genitalia; vitelline follicles 17–32 (23 ± 4.8; 6, 18) long by 39–54 (45 ± 4.4; 6, 18) wide. Uterus medial, saccate, ventral to vagina, extending anteriorly from ovarian isthmus to near anterior margin of proglottid. Excretory vessels 4, arranged in 1 dorsal and 1 ventral pair on each lateral margin of proglottid. Oncospheres not observed.

Type and only known host

Sympterygia brevicaudata (Cope) (Rajiformes: Arhynchobatidae Fowler).

Type locality

Viña del Mar, Chile (32°53′22.9″S, 71°31′32.1″W).

Additional localities

None.

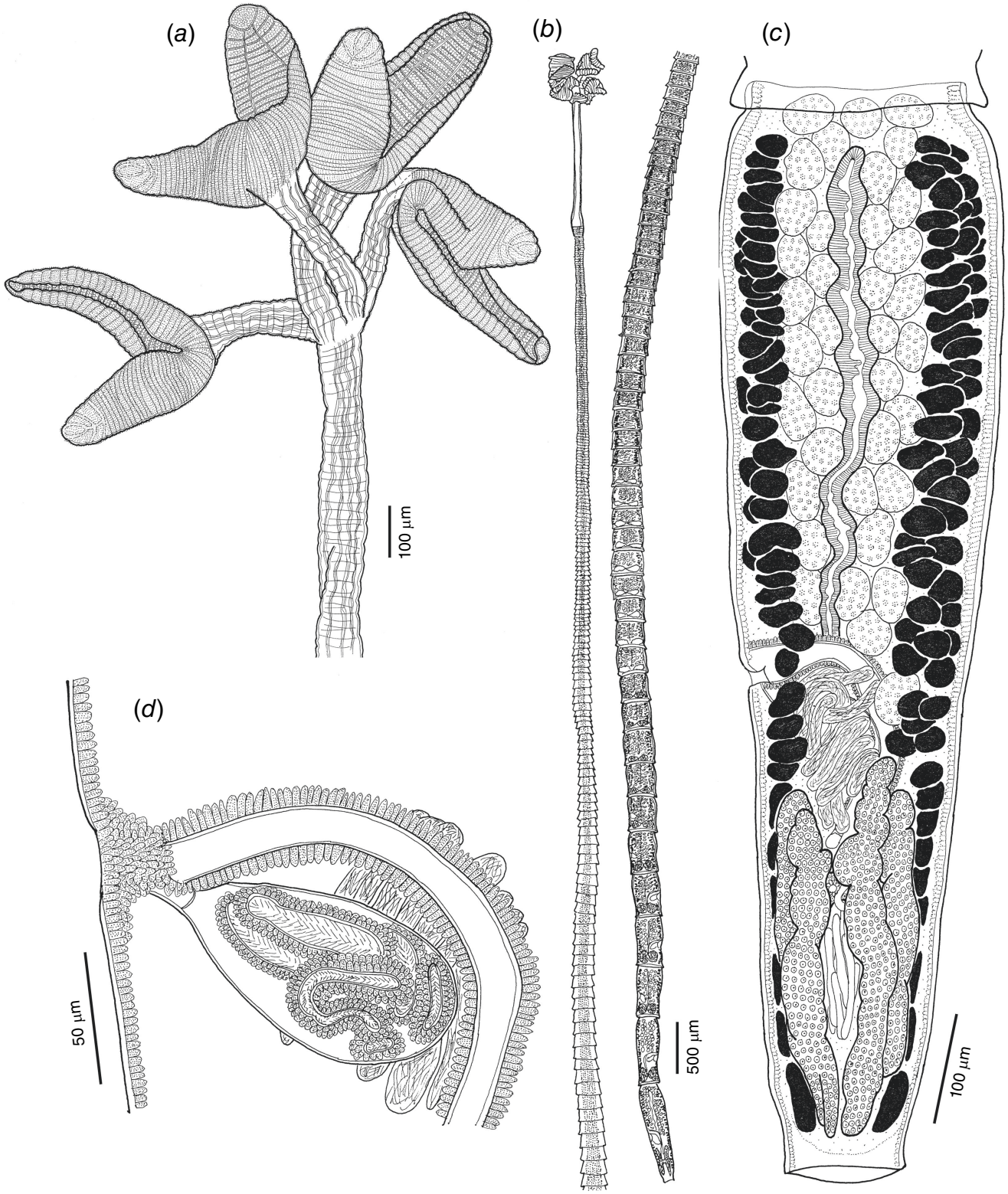

Fig. 4. Illustrations of *Semiorbiseptum beitae*, sp. nov. (*a*) Scolex (paratype, USNM number 1707281). (*b*) Whole worm (holotype, MNHNCL number PLAT-15065). (*c*) Terminal mature proglottid (holotype, MNHNCL number PLAT-15065). (*d*) Detail of terminal genitalia (paratype, LRP number 9815).

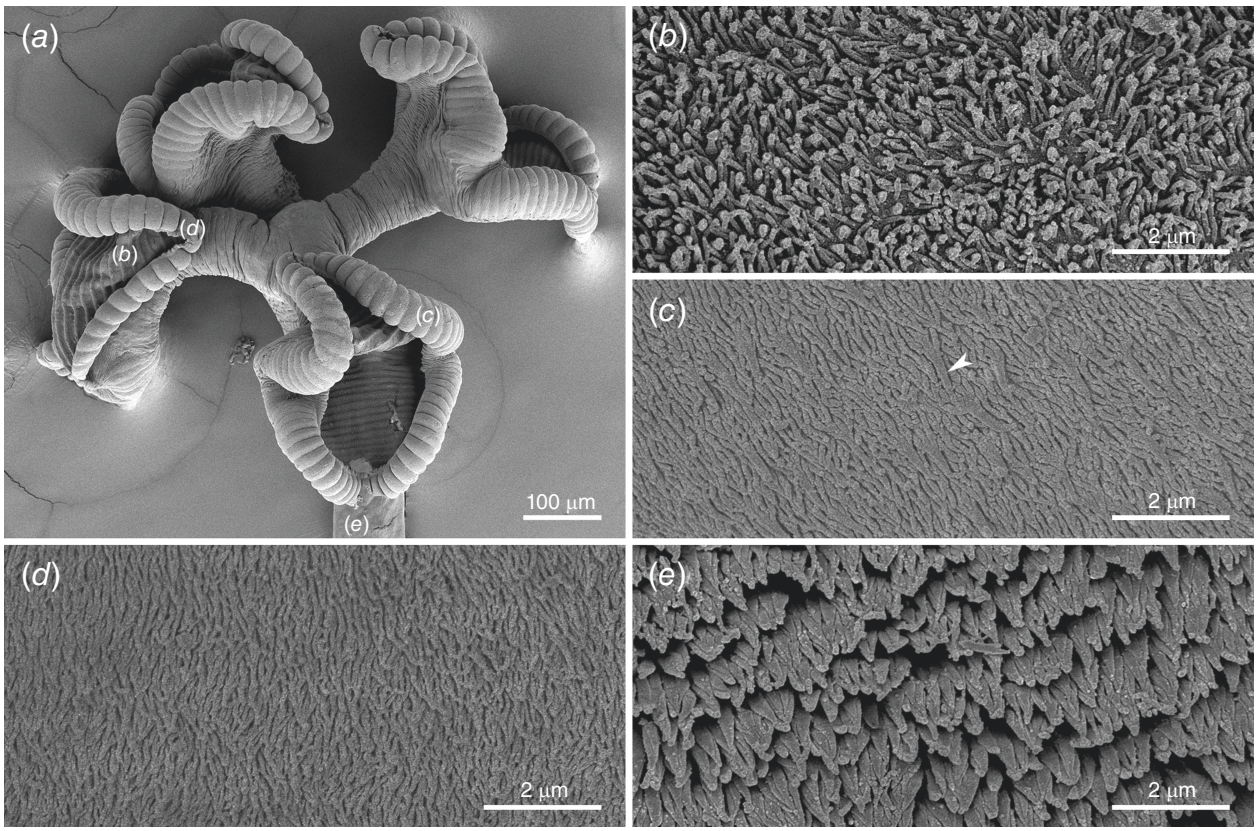

Fig. 5. Scanning electron micrographs of *Semiorbiseptum beitae*, sp. nov. (*a*) Scolex, the location of details in micrographs *b–e* are indicated in panel *a*. (*b*) Distal surface of bothridium covered with acicular filitriches. (*c*) Proximal surface of bothridium covered with acicular filitriches interspersed with small, sparsely distributed gladiate spinitriches (arrow). (*d*) Proximal surface of apical sucker covered with acicular filitriches. (*e*) Cephalic peduncle covered with small, densely distributed gladiate spinitriches.

Site of infection

Spiral intestine.

Type specimens examined

Holotype (MNHNCL number PLAT-15065) and 3 paratypes (MNHNCL numbers PLAT-15066–PLAT-15068); 4 paratypes (USNM numbers 1707279–1707282); 3 paratypes (LRP numbers 9815–9817) and 2 SEM vouchers (LRP numbers 11064–11065). Scoleces prepared for SEM retained with JNC at the University of Connecticut.

Sequence data

GenBank numbers PP375518 (VB121, hologenophore LRP number 9818), PP375519 (VB122, hologenophore LRP number 9819) and PP375520 (VB126, hologenophore LRP number 9820).

Etymology

This name honors biologist Beatriz (Beita) Salgado from Viña del Mar, Chile for assistance with the collection of the type specimens of this species.

Provisional names

New genus 23, sp. nov. 2 of Bueno (2018).

Remarks

Semiorbiseptum beitae, sp. nov. differs conspicuously from *S. alfredoi*, *S. chilensis*, *S. ivanovae*, *S. kirchneri*, *S. mariae* and *S. scobinae* in possessing many more loculi per bothridium (53–60 *v.* 12–16, 36, 12–14, 13–15, 19–23 and 15–17 respectively). There is a further difference from all of these species except *S. chilensis* in the configuration of the loculi and the septa. More specifically, this species lacks the semicircular septa in the central region of the bothridia seen in *S. alfredoi*, *S. mariae* and *S. scobinae*. Unlike *S. ivanovae* and *S. kirchneri*, which possess only transverse septa, the posterior region of the bothridia in *S. beitae*, sp. nov. possesses a short, medial longitudinal septum forming two tandem pairs of loculi immediately anterior to the terminal loculus. The species differs further from *S. chilensis* in bearing a shorter cephalic peduncle (692–1899 *v.* 2500) and *S. scobinae* in bearing more testes (27–37 *v.* 18–24). There are fewer proglottids than in *S. leiblei* (260–289 *v.* 310) and more proglottids than in *S. yakiae* (260–289 *v.* 203–239).

Each lateral band of vitelline follicles consisting of one dorsal and one ventral column of relatively large vitelline follicles in *S. beitae*, sp. nov. further distinguishes this species from *S. leiblei* in which each band consists of multiple columns of relatively small vitelline follicles.

Semiorbiseptum marquesi Bueno, Trevisan & Caira, sp. nov.

(Fig. 6, 7.)

ZooBank: urn:lsid:zoobank.org:act:1D68CA58-D136-40E8-8D1A-516FC7B09C23

Description

Based on 2 complete mature worms, 1 complete immature worm and 1 scolex observed with SEM.

Worms euapolytic, 27–53 mm ($N = 2$) long, greatest width at level of scolex; 251–283 ($N = 2$) proglottids per worm. Scolex 3641–6404 ($N = 3$) long by 730–986 ($N = 3$) wide; consisting of 4 stalked bothridia (Fig. 6*b*) and pronounced cephalic peduncle (Fig. 6*a*). Bothridia with apical sucker, 964–1093 ($N = 3$) long by 361–383 ($N = 3$) wide; each bothridium divided by transverse septa into 41–43 ($N = 2$) loculi; central region without semicircular septa; posterior region with short, medial longitudinal septum forming 2 tandem pairs of loculi immediately anterior to single terminal loculus; apical sucker 51–80 ($N = 2$, $n = 3$) long by 69–85 ($N = 2$, $n = 3$) wide. Cephalic peduncle conspicuous, 2821–5386 ($N = 3$) long by 205–299 ($N = 3$) wide at posterior end. Distal surfaces of loculi covered with acicular filitriches interspersed with small gladiate spinitriches (Fig. 7*b*); distal surfaces of septa covered with acicular filitriches interspersed with small, densely distributed gladiate spinitriches (Fig. 7*c*); distal surface of apical sucker covered with acicular filitriches interspersed with small gladiate spinitriches (Fig. 7*d*); proximal surfaces of bothridia covered with acicular filitriches (Fig. 7*g*); proximal surface of central portion of posterior region of bothridia covered with acicular filitriches interspersed with small, very sparsely distributed gladiate spinitriches (Fig. 7*h*); proximal surface of posteriormost loculus covered with acicular filitriches interspersed with small, sparsely distributed gladiate spinitriches (Fig. 7*f*); cephalic peduncle covered with small, densely distributed gladiate spinitriches (Fig. 7*e*).

Proglottids craspedote. Immature proglottids 238–265 ($N = 2$) in number, wider than long, becoming longer than wide with maturity. Mature proglottids 13–18 ($N = 2$) in number, longer than wide; terminal mature proglottid 786–818 ($N = 2$) long by 479–496 ($N = 2$) wide, length:width ratio 1.58–1.71 ($N = 2$): 1; gravid proglottids not observed. Genital pores marginal, 49–51% ($N = 2$) of proglottid length from posterior margin in terminal proglottid, irregularly alternating. Testes 30–39 ($N = 2$) in number, 31–46 long ($N = 2$; $n = 12$) by 61–76 ($N = 2$; $n = 12$) wide, 1 layer deep, arranged in 3–4 irregular columns, extending from anterior margin of proglottid to level of cirrus sac on poral side and to level of ovary on aporal side (Fig. 6*c*). Vas deferens highly coiled at level of cirrus sac, extending posteriorly to level of ovarian bridge. Cirrus sac (Fig. 6*d*) thin-walled, pyriform, slightly tilted posteriorly, containing coiled cirrus, 154–159 ($N = 2$) long by 78–95 ($N = 2$) wide; cirrus armed with spinitriches. Vagina thick-walled, weakly sinuous, extending from ootype along medial line of proglottid to level of cirrus sac, extending along anterior margin of cirrus sac to open into genital atrium anterior to cirrus; vaginal sphincter lacking; seminal receptacle not observed. Ovary at posterior end of proglottid, with lobed margins, H-shaped in frontal view, tetralobed in cross-section, symmetrical, 206–234 ($N = 2$) long by 323–339 ($N = 2$) wide. Mehlis' gland posterior to ovarian isthmus. Vitellarium follicular; follicles arranged in 2 lateral bands; each band consisting of 1 dorsal and 1 ventral column of follicles, extending throughout length of proglottid, interrupted ventrally by terminal genitalia; vitelline follicles 18–25 ($N = 2$; $n = 6$) long by 61–72 ($N = 2$; $n = 6$) wide. Uterus medial, saccate, ventral to vagina, extending anteriorly from ovarian isthmus to near anterior margin of proglottid. Excretory vessels 4, arranged in 1 dorsal and 1 ventral pair on each lateral margin of proglottid. Oncospheres not observed.

Type and only known host

Sympterygia brevicaudata (Cope) (Rajiformes: Arhynchobatidae Fowler).

Type locality

Viña del Mar, Chile (32°53′22.9″S, 71°31′32.1″W).

Additional localities

None.

Site of infection

Spiral intestine.

Type specimens examined

Holotype (MNHNCL number PLAT-15069); one paratype (USNM number 1707283); one paratype and one SEM voucher (LRP numbers 9812–9813). Scolex prepared for SEM retained with JNC at the University of Connecticut.

Sequence data

GenBank number PP375524 (VB123, hologenophore LRP number 9814).

Etymology

This name honours parasitologist and evolutionary biologist Fernando P. L. Marques for providing specimens for this study, for his contributions to the systematics of elasmobranch tapeworms and his continued support of the first two authors.

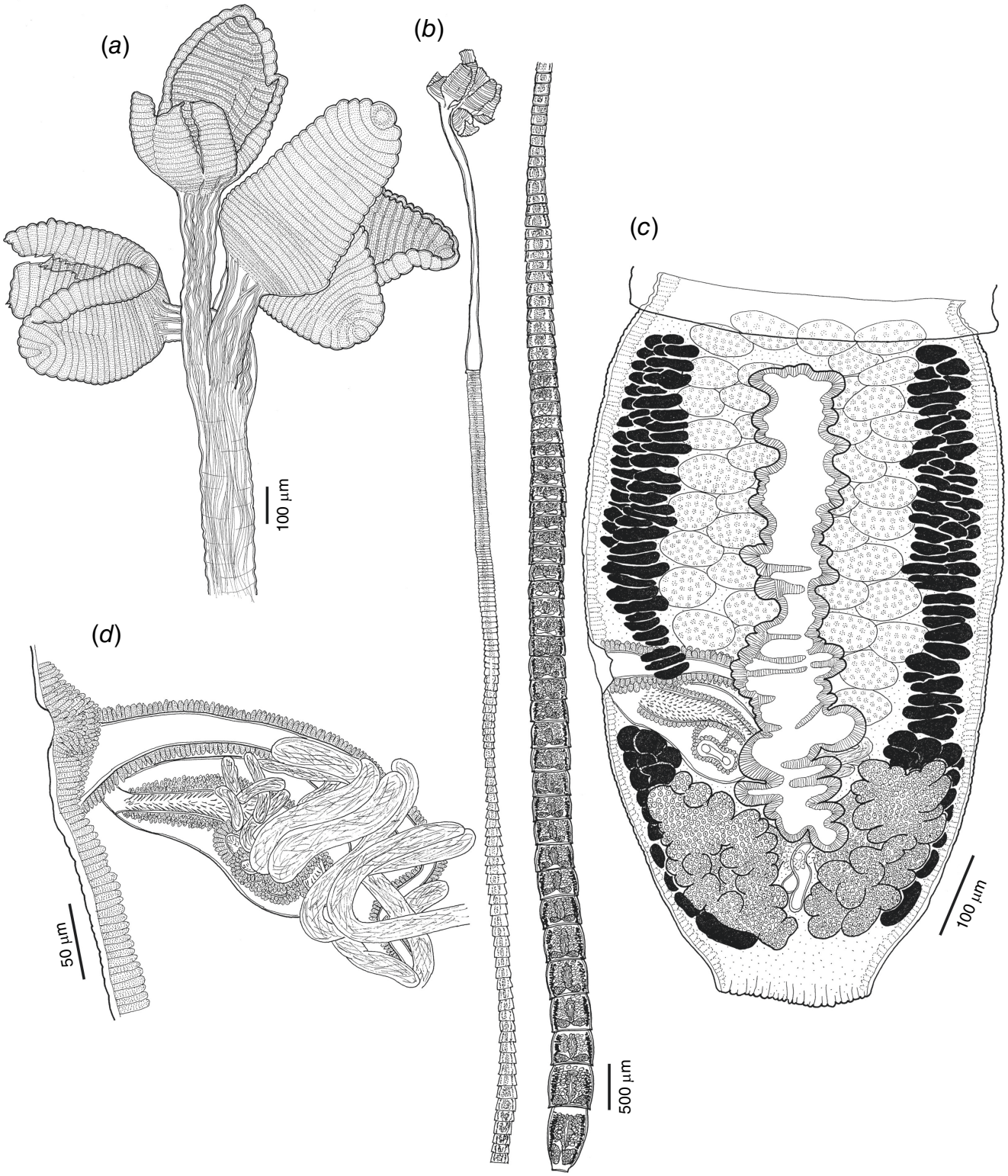

Fig. 6. Illustrations of *Semiorbiseptum marquesi*, sp. nov. (*a*) Scolex (paratype, USNM number 1707283). (*b*) Whole worm (holotype, MNHNCL number PLAT-15069). (*c*) Terminal mature proglottid (paratype, LRP number 9812). (*d*) Detail of terminal genitalia (paratype, LRP number 9812).

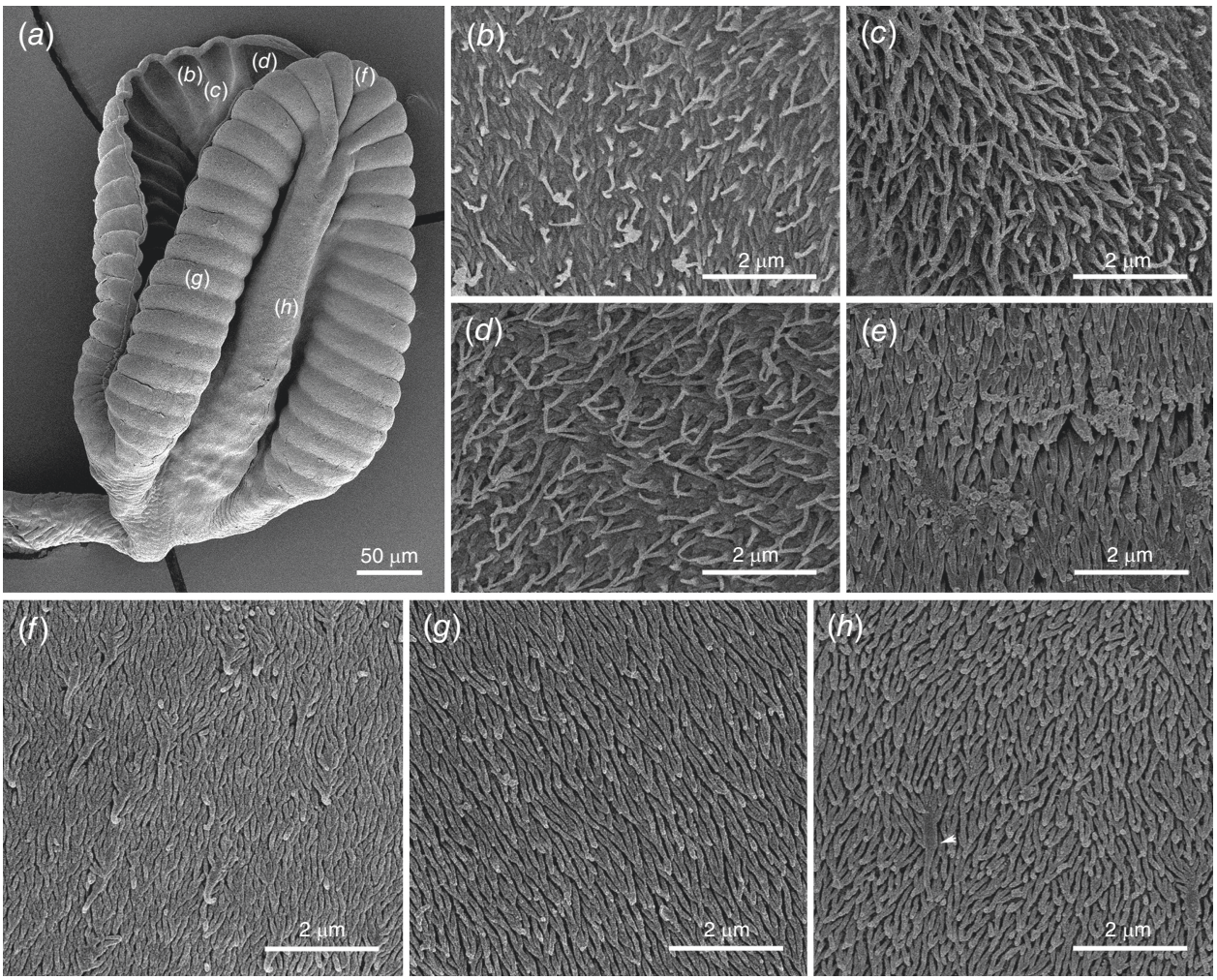

Fig. 7. Scanning electron micrographs of *Semiorbiseptum marquesi*, sp. nov. (*a*) Bothridium, the location of details in micrographs *b–d*, *f–h* are indicated in panel *a*. (*b*) Distal surface of loculus covered with acicular filitriches interspersed with small gladiate spinitriches. (*c*) Distal surface of septum covered with acicular filitriches interspersed with small, densely distributed gladiate spinitriches. (*d*) Distal surface of apical sucker covered with acicular filitriches interspersed with small gladiate spinitriches. (*e*) Cephalic peduncle covered with small, densely distributed gladiate spinitriches. (*f*) Proximal surface of posteriormost loculus covered with acicular filitriches interspersed with small, sparsely distributed gladiate spinitriches. (*g*) Proximal surface of bothridium covered with acicular filitriches. (*h*) Proximal surface of central portion of posterior region of bothridium covered with acicular filitriches interspersed with small, very sparsely distributed gladiate spinitriches (arrow).

Provisional names

New genus 23, sp. nov. 1 of Bueno (2018).

Remarks

Semiorbiseptum marquesi, sp. nov. is a larger worm (27–53 *v*. 20.8–26 mm), with longer bothridia (964–1093 *v*. 633–810) and a longer cephalic peduncle (2821–5386 *v*. 692–1899) than *S. beitae*. This species differs conspicuously from *S. alfredoi*, *S. chilensis*, *S. ivanovae*, *S. kirchneri*, *S. mariae* and *S. scobinae* in possessing many more loculi per bothridium (41–43 *v*. 13–16, 36, 12–14, 13–15, 19–23 and 15–17 respectively). There is a further difference from all of these species except *S. chilensis* in the configuration of the loculi and septa. More specifically, the semicircular septa at the centre of the bothridia that are present in *S. alfredoi*, *S. mariae* and *S. scobinae* are lacking. Unlike *S. ivanovae* and *S. kirchneri*, which possess only transverse septa, the posterior region of the bothridia in *S. marquesi*, sp. nov. possesses a short, medial longitudinal septum forming two tandem pairs of loculi immediately anterior to the terminal loculus. *Semiorbiseptum marquesi* differs further from *S. scobinae* in bearing more testes (30–39 *v*. 18–24), differs from *S. leiblei* in possessing fewer proglottids (251–283 *v*. 310), and differs from *S. yakiae* in possessing more proglottids (251–283 *v*. 203–239). The configuration of the vitelline follicles further distinguishes *S. marquesi*, sp. nov. from *S. leiblei*; whereas each lateral band of vitelline follicles in the former species consists of two dorsal and two ventral

columns of relatively large vitelline follicles, those of the latter species each consists of multiple columns of relatively small vitelline follicles. *Semiorbiseptum marquesi* also bears bothridia that are considerably longer than those observed in *S. yakiae* (964–1093 *v*. 335–690).

Genus ***Semiorbiseptum*** Franzese & Ivanov, 2020 amended

Ivanovcestus Franzese, Montes, Shimabukuru & Arredondo, 2024

Diagnosis

Rhinebothriidea: **Escherbothriidae**. Worms euapolytic, proglottids craspedote, non-laciniate. Scolex with 4 bothridia and **pronounced** cephalic peduncle. Bothridia stalked, with conspicuous anterior-posterior orientation, **bearing apical sucker and numerous transverse septa; central region with or without semicircular septa; posterior region with or occasionally without short, medial longitudinal septum forming 2 tandem pairs of loculi immediately anterior to single terminal loculus.** Testes in 2 **or more columns** anterior to cirrus sac, 1 layer deep in cross-section. Genital pores lateral, irregularly alternating. Cirrus covered with spinitriches. Ovary **H-shaped in frontal view, tetralobed in cross-section,** at posterior end of proglottid. Vagina opening anteriorly to cirrus sac into genital atrium. Vitellarium follicular; vitelline follicles in 2 lateral bands. Uterus saccate, medioventral. Two pairs of excretory vessels. Parasites of *Psammobatis*, *Sympterygia*, *Rioraja* and *Atlantoraja* (Rajiformes: Arhynchobatidae).

Type species: *Semiorbiseptum mariae* Franzese & Ivanov, 2020.

Additional species: *Semiorbiseptum alfredoi* Franzese & Ivanov, 2020, *Semiorbiseptum beitae*, sp. nov., *Semiorbiseptum chilensis* (Euzet & Carvajal, 1973), comb. nov., *Semiorbiseptum ivanovae* (Franzese, 2021), comb. nov., *Semiorbiseptum kirchneri* (Franzese & Ivanov, 2021), comb. nov., *Semiorbiseptum leiblei* (Euzet & Carvajal, 1973), comb. nov., *Semiorbiseptum marquesi*, sp. nov., *Semiorbiseptum scobinae* (Euzet & Carvajal, 1973), comb. nov. and *Semiorbiseptum yakiae* (Franzese, Montes, Shimabukuro & Arredondo, 2024), comb. nov.

Remarks

Semiorbiseptum was erected by Franzese and Ivanov (2020) to house *S. alfredoi* and *S. mariae*, both of which parasitise skates in the genus *Psammobatis*. Among the features used to justify the establishment of this genus was the presence of a unique arrangement of semicircular septa in the central region of the bothridia, along with a short medial longitudinal septum at the posterior end of the bothridia. Our phylogenetic analysis and morphological studies, however, indicate that the presence of semicircular septa is not diagnostic of the genus but instead appears to be unique to members of *Semiorbiseptum* that parasitise skates in the genus *Psammobatis* (i.e. *S. mariae*, *S. alfredoi* and *S. scobinae*). However, all three of these species share the presence of a short medial longitudinal septum associated with one single terminal loculus and two tandem pairs of loculi at the posterior region of the bothridia with five other species of *Semiorbiseptum*, the exceptions being *S. kirchneri* and *S. ivanovae*.

The diagnosis of the genus *Semiorbiseptum* provided by Franzese and Ivanov (2020) is amended above to accommodate the description of two new species and transfer of six species to the genus. Modifications are indicated in bold. One of the features most affected by these taxonomic actions is recognition that an apical sucker is present on each bothridium in all 10 members of the genus. *Semiorbiseptum beitae*, *S. marquesi*, *S. scobinae* and *S. yakiae* were originally described as possessing apical suckers. Franzese *et al.* (2024) revised the interpretation of this feature in *S. chilensis* and *S. leiblei* from absent to present when these species were transferred to *Ivanovcestus*. We would argue that evidence for the presence of apical suckers was also provided in images presented in recent papers treating *S. alfredoi* (see Franzese and Ivanov 2020, fig. 6C and 7B), *S. ivanovae* (see Franzese and Ivanov 2021, fig. 5C and 6A), *S. kirchneri* (see Franzese and Ivanov 2021, fig. 1C, 2A) and *S. mariae* (see Franzese and Ivanov 2020, fig. 2B, 2C). As a consequence, we believe this feature also characterises the genus. Rather than describing the cephalic peduncle of the members of *Semiorbiseptum* as merely present, we argue that this is pronounced and serves as an additional diagnostic feature of this genus. We have also modified the description of the septa and loculi in part to emphasise the presence of the short medial septum forming two tandem pairs of loculi on the posterior margin of the bothridia in most species. Although Franzese and Ivanov (2020, 2021) described the configuration of the septal muscle bundles in four members of the genus in excellent detail, the presence of this configuration has yet to be investigated in the remaining six species. As a consequence, we have removed mention of this feature until it is confirmed in the remaining members of the genus. Similarly, description of shape of the eggs has been removed from the generic diagnosis until this has been confirmed in species beyond *S. mariae* (see Franzese and Ivanov 2020). The number of columns of testes has been expanded to accommodate all species currently housed in the genus. Finally, the description of the insertion of the vas deferens in the cirrus sac has been removed until this can be verified in all members of the genus.

Escherbothrium molinae Berman & Brooks, 1994 amended

(Fig. 8.)

The description of *Escherbothrium molinae* provided by Berman and Brooks (1994) is amended to include the following information, based on holotype, 10 complete

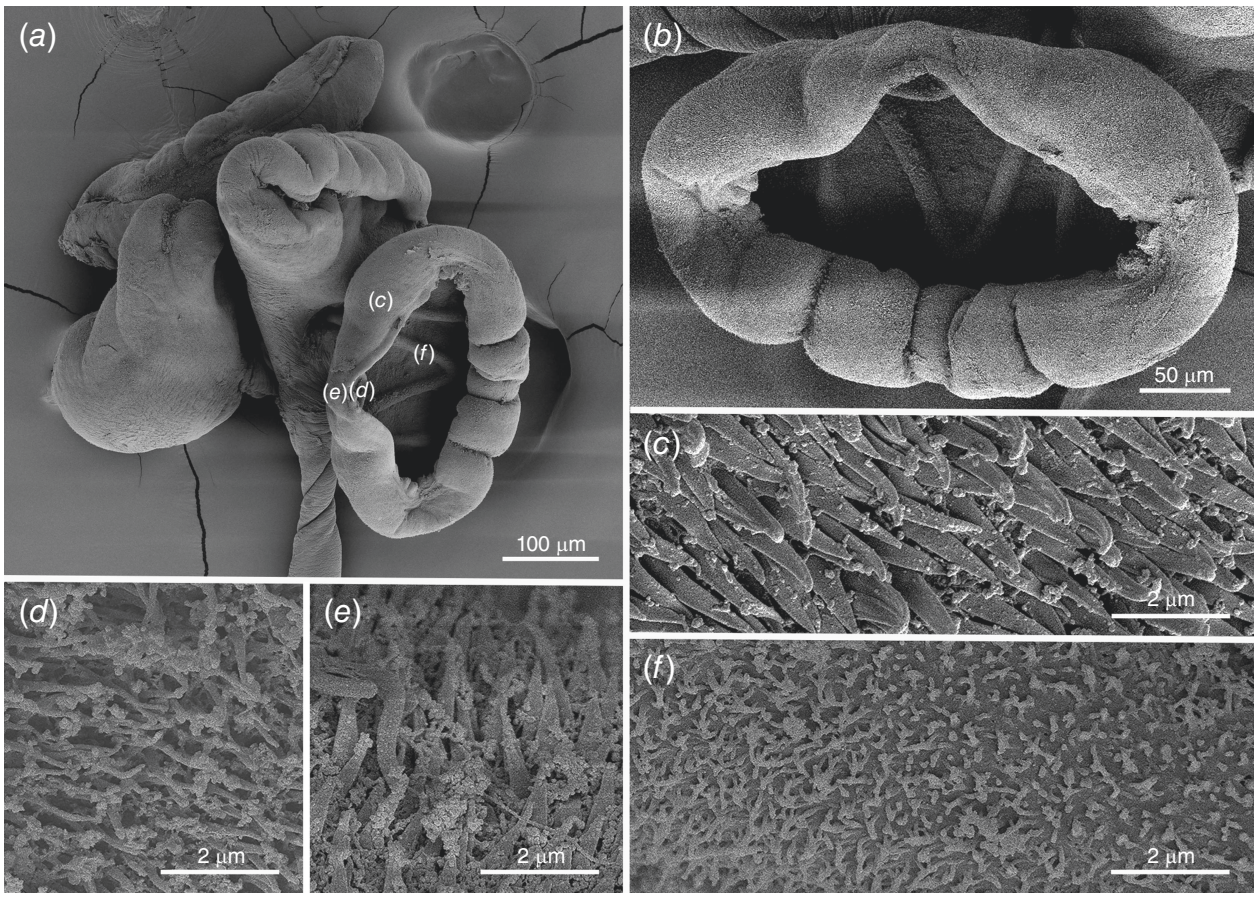

Fig. 8. Scanning electron micrographs of *Escherbothrium molinae* Berman & Brooks, 1994. (*a*) Scolex, the location of details in micrographs *c–f* are indicated in panel *a*. (*b*) Detail of bothridium. (*c*) Proximal surface of bothridium covered with densely distributed gladiate spinitriches interspersed with capilliform filitriches. (*d*) Distal surface of apical sucker covered with densely distributed capilliform filitriches. (*e*) Proximal surface of apical sucker covered with densely distributed gladiate spinitriches interspersed with capilliform filitriches. (*f*) Distal surface of bothridium covered with acicular filitriches.

mature voucher worms, 1 paragenophore and 2 scoleces observed with SEM.

Bothridia with apical sucker; each bothridium divided into loculi by 2 lateral longitudinal septa and 2 medial diagonal septa fused at cross point, delimiting 1 large anterior triangular loculus and 1 small posterior triangular loculus. Anterior triangular loculus at least 85–195 (128 ± 27.9; 11, 28) wide; posterior triangular loculus 53–79 (68 ± 9.2; 5, 7) long by 48–68 (55 ± 8.2; 5, 7) wide. Ovary H-shaped in frontal view, tetralobed in cross-section. Vaginal sphincter absent. Proximal surfaces of bothridia (Fig. 8*c*) and apical sucker (Fig. 8*e*) covered with densely distributed gladiate spinitriches interspersed with capilliform filitriches; distal surfaces of bothridia (Fig. 8*f*) covered with acicular filitriches; distal surface of apical sucker (Fig. 8*d*) covered with densely distributed capilliform filitriches.

Type and only known host

Urotrygon chilensis (Günther) (Myliobatiformes: Urotrygonidae McEachran, Dunn & Miyake).

Type locality

Costa de Pajaros, Gulf of Nicoya, Costa Rica.

Additional localities

Punta Morales, Gulf of Nicoya, Costa Rica; Salina Cruz, Oaxaca, Mexico (16°09′29.5″N 95°11′26.5″W).

Type specimens examined

Holotype (USNM number 1379291).

Site of infection

Spiral intestine.

Voucher specimens deposited

Seven voucher specimens from the type locality donated by D. Brooks (LRP numbers 11050–11056); three voucher specimens from Mexico (LRP numbers 11057–11059); one SEM

voucher (LRP number 11061); scoleces prepared for SEM retained with JNC at the University of Connecticut.

Sequence data

GenBank numbers PP375516 (DA-29, voucher image LRP number 11062), PP375517 (DA-30, voucher image LRP number 11063); paragenophore (LRP number 11060).

Remarks

The original description of this species includes SEM images of the scolex. However, detailed information on the microthrix pattern on the bothridial surfaces is lacking. The configuration of microtriches is often taxonomically informative, therefore we have amended the original description to include this information. In addition, although the original description states that the ovary in *E. molinae* is 'bilobed, V-shaped in frontal view' (Berman and Brooks 1994, p. 775), examination of the holotype and voucher specimens suggests that the ovary is H-shaped in frontal view. Also, we believe the original report of the presence of a vaginal sphincter in *E. molinae* to be in error. This feature is not represented in the original illustrations (Berman and Brooks 1994, p. 776, fig. 3 and 4) and we did not observe a vaginal sphincter in any of the type or voucher material examined. Measurements of the posterior triangular loculus were added to the description to increase the number of characters of potential taxonomic value. Our new material, collected off the coast of Oaxaca, Mexico, extends the distribution of *E. molinae* into the waters off North America.

Escherbothrium cielochae Bueno, Trevisan & Caira, sp. nov.

(Fig. 9, 10.)

ZooBank: urn:lsid:zoobank.org:act:825FAC70-36D5-475D-A0FB-60222882FE9E

Description

Based on 13 complete mature worms and 2 scoleces observed with SEM.

Worms euapolytic, 4.4–13.4 (8 ± 2.9; 13) mm long, greatest width at level of scolex; 25–53 (41 ± 8; 13) proglottids per worm. Scolex 486–1018 (733 ± 168.7; 11) long by 719–1099 (910 ± 129; 11) wide, consisting of 4 cup-shaped, weakly stalked bothridia (Fig. 9*b*) and cephalic peduncle (Fig. 9*a*). Bothridia with apical sucker, 252–405 (358 ± 38.8; 13; 26) long by 510–753 (653 ± 69.1; 13; 29) wide; each bothridium divided into loculi by 2 lateral longitudinal septa and 2 medial diagonal septa fused at cross point, delimiting 1 large anterior triangular loculus and 1 small posterior triangular loculus. Anterior triangular loculus at least 111–232 (152 ± 33.6; 12, 19) wide; posterior triangular loculus 112–181 (137 ± 25.3; 6, 7) long by 82–128 (99 ± 15.2; 6, 7) wide; apical sucker 61–108 (82 ± 14.9; 11; 23) long by 53–103 (80 ± 14; 11; 23) wide. Cephalic peduncle inconspicuous, 61–456 (236 ± 126.4; 13) long by 73–129 (105 ± 17.9; 13) wide. Proximal surfaces of bothridia (Fig. 10*d*) and apical sucker (Fig. 10*f*) covered with densely distributed capilliform filitriches interspersed with large gladiate spinitriches; proximal surfaces near bothridial margins (Fig. 10*e*) covered with densely distributed capilliform filitriches interspersed with sparsely distributed gladiate spinitriches, gradually replaced with papilliform filitriches toward the margin; distal surfaces of bothridia (Fig. 10*b*) and posteriormost loculus (Fig. 10*c*) covered with acicular filitriches interspersed with small gladiate spinitriches.

Proglottids slightly craspedote. Immature proglottids 24–51 (40 ± 8; 13) in number, wider than long, becoming longer than wide with maturity. Mature proglottids 1–3 (2 ± 0.7; 13) in number, longer than wide (Fig. 8*b*), terminal mature proglottid 519–888 (698 ± 107.7; 13) long by 176–272 (220 ± 28.6; 13) wide, length:width ratio 2.1–4.2 (3 ± 0.7; 13): 1; gravid proglottids not observed. Genital pores marginal, 38–52% (44 ± 4; 13) of proglottid length from posterior margin in terminal mature proglottid, irregularly alternating. Testes 21–30 (25 ± 2.1; 13; 28) in number, 19–54 long (32 ± 7; 13; 62) by 23–70 (46 ± 9.3; 13; 62) wide, 1 layer deep, arranged in 2 regular columns extending from anterior margin of proglottid to level of cirrus sac (Fig. 9*c*). Vas deferens highly coiled at level of cirrus sac. Cirrus sac (Fig. 9*d*) thin-walled, pyriform, slightly tilted posteriorly, containing coiled cirrus, 35–52 (43 ± 5.6; 9) long by 52–77 (64 ± 8.6; 9) wide; cirrus armed with spinitriches. Vagina thick-walled, weakly sinuous, extending from ootype along medial line of proglottid to level of cirrus sac, extending along anterior margin of cirrus sac to open into genital atrium anterior to cirrus; vaginal sphincter lacking; seminal receptacle lacking. Ovary near posterior end of proglottid, with smooth margins, H-shaped in frontal view, tetralobed in cross-section, symmetrical; 151–332 (239 ± 49.4; 13; 26) long by 110–190 (139 ± 25.6; 13) wide. Mehlis' gland posterior to ovarian isthmus. Vitellarium follicular; follicles in 2 lateral bands; each band consisting of 1 dorsal and 1 ventral column of follicles, extending from slightly posterior of anterior margin of testicular field to posterior margin of proglottid, interrupted ventrally by terminal genitalia; vitelline follicles 12–25 (16 ± 3.1; 11; 34) long by 20–45 (34 ± 6.1; 11; 34) wide. Uterus medial, saccate, ventral to vagina, extending anteriorly from ovarian isthmus to near anterior margin of proglottid. Excretory vessels 4, arranged in 1 dorsal and 1 ventral pair on each lateral margin of proglottid. Oncospheres not observed.

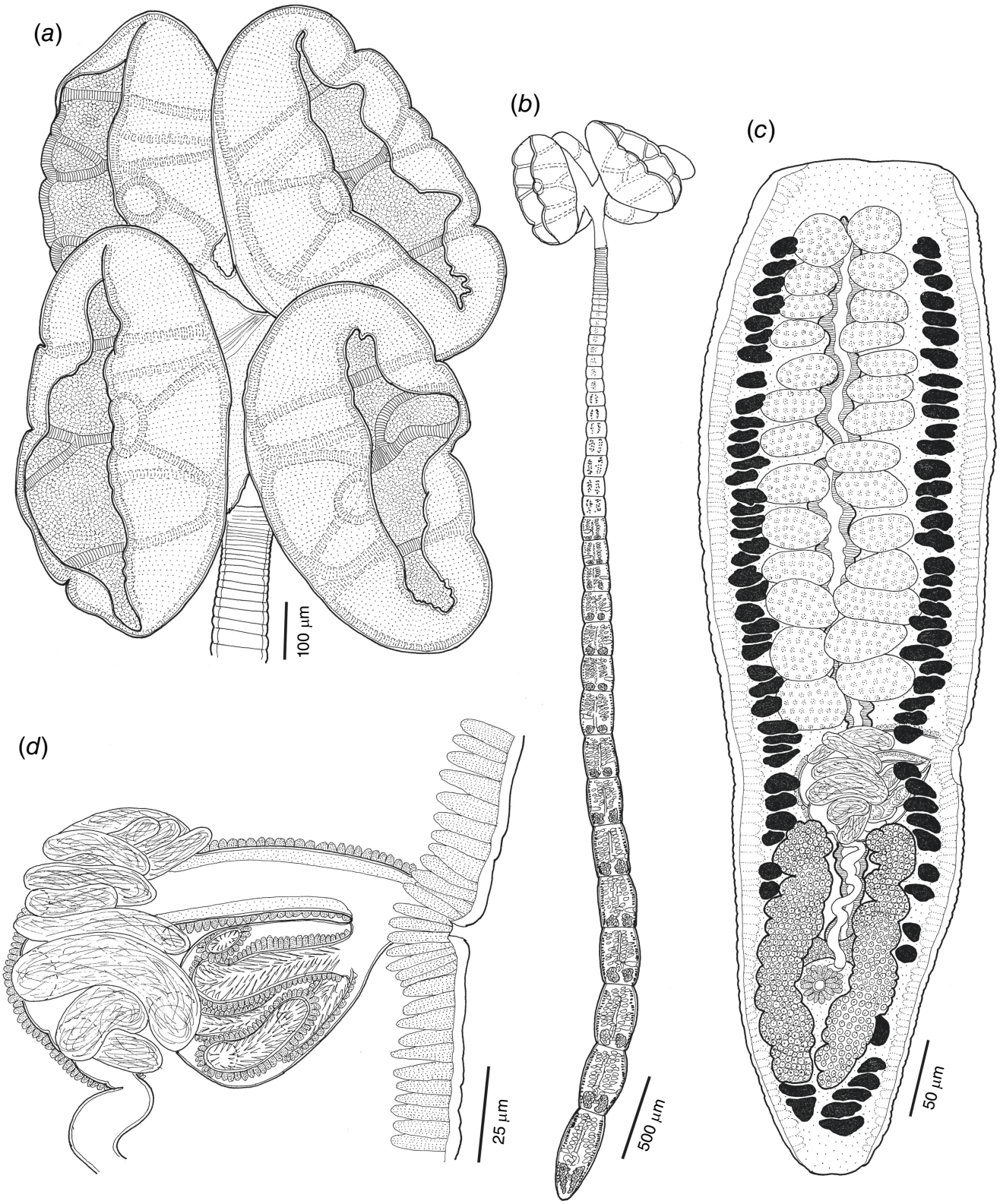

Fig. 9. Illustrations of *Escherbothrium cielochae*, sp. nov. (*a*) Scolex (paratype, LRP number 11047). (*b*) Whole worm (paratype, CNHE number 12862). (*c*) Terminal mature proglottid (holotype, USNM number 1707275). (*d*) Detail of terminal genitalia (holotype, USNM number 1707275).

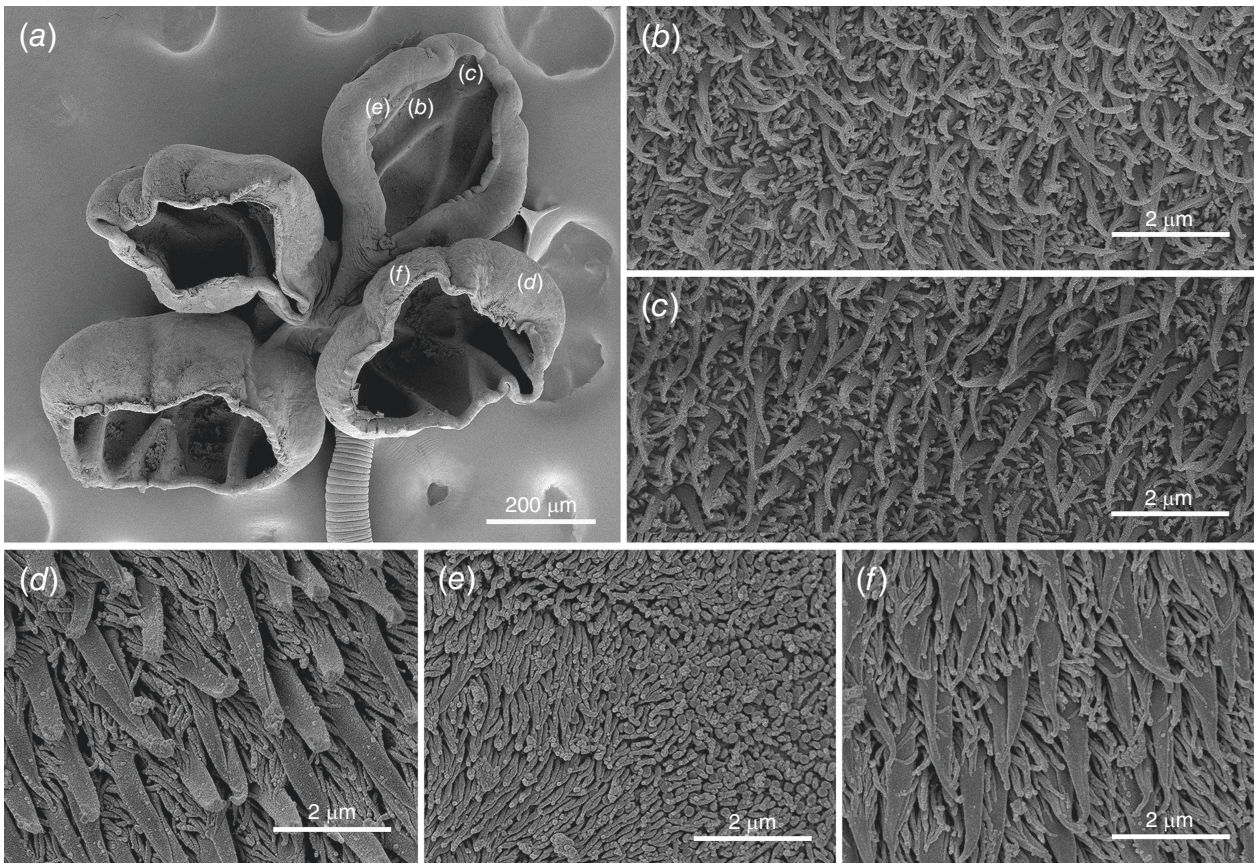

Fig. 10. Scanning electron micrographs of *Escherbothrium cielochae*, sp. nov. (*a*) Scolex, the location of details in micrographs *b–f* are indicated in panel *a*. (*b*) Distal surface of bothridium covered with acicular filitriches interspersed with small gladiate spinitriches. (*c*) Distal surface of posteriormost loculus covered with acicular filitriches interspersed with small gladiate spinitriches. (*d*) Proximal surface of bothridium covered with densely distributed capilliform filitriches interspersed with large gladiate spinitriches. (*e*) Proximal surface near bothridial margin covered with densely distributed acicular filitriches, gradually replaced with papilliform filitriches toward the margin. (*f*) Proximal surface of apical sucker covered with densely distributed capilliform filitriches interspersed with large gladiate spinitriches.

Type and only known host

Urotrygon rogersi (Jordan & Starks) (Myliobatiformes: Urotrygonidae McEachran, Dunn & Miyake).

Type locality

Gulf of Papagayo, Costa Rica, Pacific Ocean (10°42′29.5″N, 85°40′9.2″W).

Additional locality

Puerto Escondido, Oaxaca, Mexico, Pacific Ocean (15°51′36.7″N, 97°3′44.0″W).

Site of infection

Spiral intestine.

Type specimens examined

Holotype (USNM number 1707275) and three paratypes (MZUCR numbers PP-051–PP-053); three paratypes (CNHE numbers 12860–12862); three paratypes (USNM numbers 1707276–1707278): three paratypes (LRP numbers 11047–11049). Scoleces prepared for SEM retained with JNC at the University of Connecticut.

Sequence data

GenBank number KM658197 (hologenophore LRP number 8519).

Etymology

This name honours parasitologist Joanna Cielocha who collected the specimens of *Urotrygon rogersi* from which the type material of this species was obtained.

Provisional names

Escherbothrium sp. of Ruhnke *et al.* (2015) (host preliminarily identified as *Urotrygon aspidura* (Jordan & Gilbert)).

Remarks

Escherbothrium cielochae, sp. nov. differs from *E. molinae* in having a longer (112–181 *v*. 53–79) and wider (82–128 *v*. 48–68) posterior triangular loculus. In addition, whereas in *E. cielochae*, sp. nov. the vitelline follicles are interrupted ventrally by the terminal genitalia, that is not the case in *E. molinae*. The two species differ further in that the gladiate spinitriches on the proximal surfaces of the bothridia are sparsely arranged in *E. cielochae* but densely arranged in *E. molinae*. In addition, the distal bothridial surfaces of *E. cielochae*, sp. nov. bear small gladiate spinitriches but spinitriches are completely lacking from the distal surfaces of the bothridia of *E. molinae*.

Family **ESCHERBOTHRIIDAE** Ruhnke, Caira & Cox, 2015 amended

Type genus: *Escherbothrium* Berman & Brooks, 1994.

Additional genera: *Stillabothrium* Healy & Reyda, 2016, *Semiorbiseptum* Franzese & Ivanov, 2020.

Diagnosis

Scolex with 4 stalked bothridia, with or without cephalic peduncle; bothridia with conspicuous anterior or posterior orientation, with or without apical sucker, occasionally with marginal loculi, with facial loculi; configuration of facial loculi in anterior and posterior bothridial halves dissimilar. Myzorhynchus absent in adult stage. Postvaginal testes absent. Ovary H-shaped in frontal view, tetralobed in cross-section. Vitelline follicles interrupted or uninterrupted by ovary or terminal genitalia. Parasites of Myliobatiformes, Rajiformes and Rhinopristiformes.

Remarks

In the revised diagnosis of the Escherbothriidae presented here, terminology referring to the configuration of the facial loculi has been simplified relative to that used in previous treatments of this family (i.e. Ruhnke *et al.* 2015, 2022; Franzese *et al.* 2024). In addition, to accommodate all members of the family, the fact that the vitelline follicles may be interrupted by the terminal genitalia has been added.

Discussion

Expanding *Semiorbiseptum* to include the eight additional species treated here has enabled us to bring order to what had been an eclectic suite of rhinebothriidean taxa known to parasitise skates. Simultaneously, however, this action appears to have added a degree of disorder to the morphological features that serve to unite the members of this clade. We would argue that this is not actually the case. One of the most contentious issues is whether the structure situated on the anterior portion of each bothridium of members of *Semiorbiseptum* is an apical sucker or merely the anteriormost of many facial loculi. The controversy stems from the fact that the presence of apical suckers appears to be a highly canalised feature given that few genera include a blend of species that possess and lack apical suckers. Yet current interpretations suggest this may be the case for the newly circumscribed concept of *Semiorbiseptum*. Franzese and Ivanov (2020) considered both of the original species of *Semiorbiseptum* to lack apical suckers, whereas Franzese *et al.* (2024) considered the three species recognised in the genus *Ivanovcestus* to possess apical suckers. We believe that the case for the presence of apical suckers in all species of *Semiorbiseptum* is strong. In establishing *Ivanovcestus*, Franzese *et al.* (2024) examined type material of the two species transferred to *Ivanovcestus* (i.e. *I. chilensis* and *I. leiblei*), both of which were originally described as lacking apical suckers, and determined that both possess this feature. When describing *S. scobinae* (as *R. scobinae*), Euzet and Carvajal (1973, p. 785) reported this species to have 'un apical ovalaire ressemble à une ventouse'. Both of our new species also exhibit apical suckers. Based on the criterion for distinguishing a sucker from a loculus established by Caira *et al.* (1999) (i.e. a membrane bound muscular organ of attachment that is round, as opposed to any other configuration), as noted above, we believe the images included in the original descriptions of all four of the remaining species provide convincing evidence of apical suckers, despite the fact that these taxa were originally described as lacking this feature. We recognise that the distinction between an apical sucker and an anterior loculus can be challenging, especially because both are soft structures that can be highly affected by fixation, processing and mounting. Nonetheless, we argue that existing morphological evidence suggests that apical suckers are present in all 10 species of *Semiorbiseptum*.

Considerable differences in the configuration of the facial loculi across the 10 species in the revised concept of *Semiorbiseptum* also initially appear to exist. However, upon closer examination, a number of similarities emerge. The presence of semicircular septa in the central region of the bothridium was considered to be a defining feature of *Semiorbiseptum* by Franzese and Ivanov (2020). Interestingly, our discovery of semicircular septa in *S. scobinae* indicates that this feature appears to be unique to species of *Semiorbiseptum* that parasitise skates in the genus *Psammobatis*. However, both of the original members of the genus and *S. scobinae* also possess what initially appeared to be a unique condition consisting of two tandem pairs of loculi followed by a single terminal loculus on the posterior margin of each bothridium. We now know that this feature is also seen in *S. beitae*, *S. chilensis*, *S. leiblei*, *S. marquesi* and *S. yakiae*. Among the 10 species of *Semiorbiseptum*, only *S. ivanovae* and *S. kirchneri* appear to lack this feature, a fact confirmed by the excellent images provided by Franzese and Ivanov (2021) in the original

descriptions of both species. When material of *S. ivanovae* becomes available for molecular analysis, based on these features, we predict that *S. ivanovae* will be found to be sister to *S. kirchneri*, in a subclade united by possession of only transverse septa.

The expansion of *Semiorbiseptum* to include eight additional species has also revealed an interesting pattern in the host associations of this genus that may contribute to our understanding of its geographic distribution. Originally known only from two species of *Psammobatis*, the new members add a third species of *Psammobatis*, one species of *Atlantoraja* Menni, one species of *Rioraja* Whitley and three species of *Sympterygia* to the repertoire of hosts of *Semiorbiseptum*. All four of these skate genera are members of the Arhynchobatidae and occur only off the coasts of South America (Last *et al.* 2016). Eight of the nine remaining genera in the family occur in waters outside South America. More specifically, the monotypic *Pseudoraja* Bigelow & Schroeder occurs in the Caribbean Sea and seven of the eight other genera are found only in Southeast Asia and Australia. None of these eight genera are known to host species of *Semiorbiseptum*. Especially interesting is the final genus of arhynchobatids, *Bathyraja*, that includes ~12 species that occur in the waters off Central and South America, none of which have been reported to host *Semiorbiseptum*. The absence of *Semiorbiseptum* from *Bathyraja* in these regions is interesting given that Naylor *et al.* (2012) found this genus to belong to a different subclade of arhynchobatid skates from the other genera that occur off Central and South America. This suggests that host phylogeny may be playing a role in the patterns of host associations of this cestode genus. If so, we would expect that the global distribution of *Semiorbiseptum* will ultimately be determined to be restricted to Central and South America. We predict that the two species of *Atlantoraja* and five species of *Psammobatis* that occur off South America that remain to be examined will each be found to host at least one additional species of *Semiorbiseptum*. Furthermore, we believe the single species of *Sympterygia* remaining to be examined will host one to two species, bringing the total number of undescribed species of *Semiorbiseptum* to at least eight. In fact, *Sympterygia acuta* Garman was reported by Bueno (2018) to host a cestode that morphologically resembles *Semiorbiseptum* but is yet to be described. An interesting test of these generalisations will be the examination of the cestode fauna of the monotypic *Arhynchobatis* Waite, the only species of which occurs off New Zealand, because this genus appears to be closely related to *Psammobatis* and *Sympterygia* and is not part of the arhynchobatid subclade that includes *Bathyraja*.

The discovery of a second species of *Escherbothrium* in a second species of *Urotrygon* provides insight into the potential extent of the unknown diversity and morphological cohesiveness of this cestode genus. We predict that if the pattern of one species of *Escherbothrium* per host species persists, examination of the remaining nine species of *Urotrygon* (see Last *et al.* 2016; Fricke *et al.* 2023) may yield as many as nine novel species of *Escherbothrium*. To date, several studies have been conducted on the cestodes of species of *Urotrygon* other than *U. chilensis* and *U. rogersi*. The lack of reports of *Escherbothrium* in some of these studies is likely because the work was focused on investigating taxa in other cestode orders (e.g. Schaeffner 2016; Herzog and Jensen 2022). That does not, however, explain the fact that this genus was not reported in the survey work of Brooks and Mayes (1980) that included examination of 16 specimens of *Urotrygon venezuelae* Schultz. Given the distributions of *Urotrygon* species are restricted to the waters of Central and South America, the genus *Escherbothrium* is likely also restricted to these regions. Regardless of the overall diversity of this genus, the discovery of a second species confirms possession of the unusual arrangement of bothridial loculi that inspired its name that includes loculi that are triangular rather than oval or rectangular.

The host icons in Fig. 1 provide a general overview of the ordinal host associations of the six rhinebothriidean families. Not unexpectedly, the two least speciose families are associated with single batoid orders. More specifically, the single genus and five species of the Mixobothriidae parasitise only rhinopristiforms and the single genus and four species of the Anindobothriidae parasitise only myliobatiforms. At the other end of the diversity spectrum are the Rhinebothriidae that, with 9 genera and 78 species, parasitise rhinopristiforms and myliobatiforms, and the Anthocephaliidae that, with 6 genera and 35 species, parasitise rhinopristiforms and myliobatiforms, and include 1 species (*Anthocephalum wedli* Ruhnke, 2011) that parasitises a torpediniform. More intriguing are the Echeneibothriidae, whose 6 genera and 36 species parasitise only rajiforms and within that order mostly the Rajidae Bonaparte. The few exceptions parasitise species of *Bathyraja* (e.g. Campbell 1977; Wojciechowska 1991; Ivanov and Campbell 2002; Franzese *et al.* 2022), and one species has been described from *Atlantoraja castelnaui* (Miranda Ribeiro) (i.e. Ivanov and Campbell 2002). Escherbothriidae is the only other family of rhinebothriideans that includes members that parasitise rajiforms, with all 10 species of *Semiorbiseptum* parasitising skates, specifically the Arhynchobatidae. The remaining 15 species in the family parasitise rhinopristiforms and myliobatiforms. The general fidelity for different skate families seen in the echeneibothriids and escherbothriids, and the fact that echeneibothriids that parasitise arhynchobatids parasitise genera (e.g. *Bathyraja*) not known to host escherbothriids, accounts for the fact that we are unaware of any instances in which the same species of skate is parasitised by both an echeneibothriid and an escherbothriid. However, if *A. castelnaui* is found to host a species of *Semiorbiseptum* that situation would change.

Phylogenetic analyses of molecular data, particularly of the D1–D3 region of the *28S rDNA* gene, has been crucial to our understanding of the membership and familial structure

within the order Rhinebothriidea (Ruhnke *et al.* 2015; Trevisan *et al.* 2017; Herzog *et al.* 2023). However, the interrelationships among the six rhinebothriidean families remain unresolved. We note that in the tree resulting from our analysis (Fig. 1), although support for the monophyly of each family is generally high, this is not the case for any of the familial interrelationships. Perhaps not unexpectedly, partial *28S rDNA* data are insufficient to resolve these more ancient relationships with confidence. We believe the analysis of additional nuclear markers will be immensely beneficial for resolving interfamilial relationships not only within the Rhinebothriidea, but also within the many other orders of cestodes that are still in need of family level classifications based on robust phylogenetic relationships. Studies focusing on developing such markers would be of transformative importance for the systematics of all cestode orders and our understanding of patterns of evolution.

A molecular phylogenetic analysis, in combination with comparative morphological work, has greatly expanded our knowledge of the Escherbothriidae, leading to the description of a second species of *Escherbothrium* and two new species of *Semiorbiseptum*, the transfer of six species previously assigned to other rhinebothriidean genera to the genus *Semiorbiseptum* and the inclusion of *Semiorbiseptum* in the family. The Escherbothriidae now consists of 3 genera and 25 species: *Escherbothrium* with 2 species, *Semiorbiseptum* with 10 species and *Stillabothrium* with 13 species. The host associations of these genera have been clarified, with *Escherbothrium* parasitising stingrays of the genus *Urotrygon*, *Semiorbiseptum* parasitising arhynchobatid skates, and *Stillabothrium* parasitising elasmobranchs of the orders Myliobatiformes and Rhinopristiformes. The former two genera appear to be restricted to the waters off Central and South America. In contrast, *Stillabothrium* is found off Senegal and throughout the waters of South-east Asia and Australia. This study underscores the importance of integrating morphological and molecular data in adding resolution to cestode systematics. We believe our findings provide a robust foundation for future research into the evolutionary history and host associations of cestodes within the order Rhinebothriidea and beyond.

References

Berman R, Brooks DR (1994) *Escherbothrium molinae* n. gen. et n. sp. (Eucestoda: Tetraphyllidea: Triloculariidae) in *Urotrygon chilensis* (Chondrichthyes: Myliobatiformes: Urolophidae) from the Gulf of Nicoya, Costa Rica. *The Journal of Parasitology* **80**, 775–780.

Brooks D, Mayes M (1980) Cestodes in four species of euryhaline stingrays from Colombia. *Proceedings of the Helminthological Society of Washington* **47**, 22–29.

Bueno VM (2018) Skate tapeworms revisited: a modern approach. PhD dissertation, University of Connecticut, Storrs, CT, USA.

Bueno VM, Caira JN (2017) Redescription and molecular assessment of relationships among three species of *Echeneibothrium* (Rhinebothriidea: Echeneibothriidae) parasitizing the yellownose skate, *Dipturus chilensis*, in Chile. *Journal of Parasitology* **103**, 268–284. doi:10.1645/16-177

Bueno VM, Caira JN (2023) Phylogenetic relationships, host associations, and three new species of a poorly known group of "tetraphyllidean" tapeworms from elasmobranchs. *Zootaxa* **5254**, 30–50. doi:10.11646/zootaxa.5254.1.2

Caira JN, Jensen K, Healy CJ (1999) On the phylogenetic relationships among tetraphyllidean, lecanicephalidean and diphyllidean tapeworm genera. *Systematic Parasitology* **42**(2), 77–151. doi:10.1023/a:1006192603349

Caira JN, Jensen K, Waeschenbach A, Olson PD, Littlewood DTJ (2014) Orders out of chaos – molecular phylogenetics reveals the complexity of shark and stingray tapeworm relationships. *International Journal for Parasitology* **44**, 55–73. doi:10.1016/j.ijpara.2013.10.004

Campbell RA (1977) New tetraphyllidean and trypanorhynch cestodes from deep-sea skates in the western North Atlantic. *Proceedings of the Helminthological Society of Washington* **44**, 191–197.

Chervy L (2009) Unified terminology for cestode microtriches: a proposal from the International Workshops on Cestode Systematics in 2002–2008. *Folia Parasitologica* **56**, 199–230. doi:10.14411/fp.2009.025

Chevreux B, Wetter T, Suhai S (1999) Genome sequence assembly using trace signals and additional sequence information. In 'Computer Science and Biology: Proceedings of the German Conference on Bioinformatics (GCB): '99', 4–6 October 1999, Hannover, Germany. (Ed. E Wingender) pp. 45–56. (GBF-Braunschweig, Department of Bioinfrormatics)

Clopton RE (2004) Standard nomenclature and metrics of plane shapes for use in gregarine taxonomy. *Comparative Parasitology* **71**, 130–140. doi:10.1654/4151

Eudy E, Caira JN, Jensen K (2019) A new species of *Pentaloculum* (Cestoda: "Tetraphyllidea") from the Taiwan Saddled carpetshark, *Cirrhoscyllium formosanum* (Orectolobiformes: Parascylliidae). *Journal of Parasitology* **105**, 303–312. doi:10.1645/18-132

Euzet L, Carvajal JG (1973) *Rhinebothrium* (Cestoda, Tetraphyllidea) parasites de Raies du genre *Psammobatis* au Chili. *Bulletin du Muséum National D'histoire Naturelle* **3**, 778–787. [In French]

Franzese S, Ivanov VA (2020) A new genus of Rhinebothriidea from species of *Psammobatis* (Rajiformes: Arhynchobatidae) off Argentina. *Zootaxa* **4803**, 355–372. doi:10.11646/zootaxa.4803.2.7

Franzese S, Ivanov VA (2021) Two new species of *Scalithrium* (Cestoda: Rhinebothriidea) from rajiform batoids of the Argentine Sea. *Zootaxa* **5005**, 62–76. doi:10.11646/zootaxa.5005.1.4

Franzese S, Mutti LD, Tropea C, Ivanov VA (2022) Morphological study of members of the genus *Echeneibothrium* (Cestoda: Rhinebothriidea: Echeneibothriidae) from rajiform skates of the Argentine Sea and analysis of the phylogenetic relationships within the family Echeneibothriidae. *Zoologischer Anzeiger* **299**, 1–20. doi:10.1016/j.jcz.2022.05.002

Franzese S, Montes MM, Shimabukuro MI, Arredondo NJ (2024) Description of a new genus of Escherbothriidae (Cestoda: Rhinebothriidea) in species of *Sympterygia* (Rajiformes: Arhynchobatidae) from South America based on morphological and molecular evidence, with an amended diagnosis of the family. *Zoologischer Anzeiger* **308**, 35–47. doi:10.1016/j.jcz.2023.11.002

Fricke R, Eschener WN, Van der Laan R (2023) Eschmeyer's catalog of fish: genera, species, references. Available at http://researcharchive.calacademy.org/research/ichthyology/catalog/fishcatmain.asp [Verified 14 October 2023]

Hahn C, Bachmann L, Chevreux B (2013) Reconstructing mitochondrial genomes directly from genomic next-generation sequencing reads—a baiting and iterative mapping approach. *Nucleic Acids Research* **41**, e129. doi:10.1093/nar/gkt371

Healy CJ, Caira JN, Jensen K, Webster BL, Littlewood DTJ (2009) Proposal for a new tapeworm order, Rhinebothriidea. *International Journal for Parasitology* **39**, 497–511. doi:10.1016/j.ijpara.2008.09.002

Herzog KS, Caira JN, Kumar Kar P, Jensen K (2023) Novelty and phylogenetic affinities of a new family of tapeworms (Cestoda: Rhinebothriidea) from endangered sawfish and guitarfish. *International Journal for Parasitology* **53**, 347–362. doi:10.1016/j.ijpara.2023.02.007

Herzog KS, Jensen K (2018) Five new species of the tapeworm genus *Anthocephalum* (Rhinebothriidea: Anthocephaliidae) parasitizing a single species of Indo-Pacific stingray and a revised diagnosis of the genus. *Journal of Parasitology* **104**, 505–522. doi:10.1645/18-53

Herzog KS, Jensen K (2022) A synergistic, global approach to revising the trypanorhynch tapeworm family Rhinoptericolidae (Trypanobatoida). *PeerJ* **10**, e12865. doi:10.7717/peerj.12865

Herzog KS, Meininger RS, Reyda FB (2021) A new species of tapeworm in the genus *Stillabothrium* (Rhinebothriidea: Escherbothriidae) from a stingray from Borneo. *Comparative Parasitology* **88**, 34–40. doi:10.1654/1525-2647-88.1.34

Hillis DM, Bull JJ (1993) An empirical test of bootstrapping as a method for assessing confidence in phylogenetic analysis. *Systematic Biology* **42**, 182–192. doi:10.1093/sysbio/42.2.182

Ivanov VA, Campbell RA (2002) *Notomegarhynchus navonae* n. gen. and n. sp. (Eucestoda: Tetraphyllidea), from skates (Rajidae: Arhynchobatinae) in the Southern Hemisphere. *Journal of Parasitology* **88**, 340–349. doi:10.1645/0022-3395(2002)088[0340:NNNGAN]2.0.CO;2

Kalyaanamoorthy S, Minh BQ, Wong TKF, von Haeseler A, Jermiin LS (2017) ModelFinder: fast model selection for accurate phylogenetic estimates. *Nature Methods* **14**, 587–589. doi:10.1038/nmeth.4285

Katoh K, Standley DM (2013) MAFFT multiple sequence alignment software version 7: improvements in performance and usability. *Molecular Biology and Evolution* **30**, 772–780. doi:10.1093/molbev/mst010

Katoh K, Rozewicki J, Yamada KD (2019) MAFFT online service: multiple sequence alignment, interactive sequence choice and visualization. *Briefings in Bioinformatics* **20**, 1160–1166. doi:10.1093/bib/bbx108

Last PR, White WT, de Carvalho MR, Séret B, Stehmann MFW, Naylor GJP (2016) 'Rays of the World.' (Cornell University Press: Ithaca, NY, USA)

Littlewood DTJ, Curini-Galletti M, Herniou EA (2000) The interrelationships of Proseriata (Platyhelminthes: Seriata) tested with molecules and morphology. *Molecular Phylogenetics and Evolution* **16**, 449–466. doi:10.1006/mpev.2000.0802

Machado DJ, Lyra ML, Grant T (2016) Mitogenome assembly from genomic multiplex libraries: comparison of strategies and novel mitogenomes for five species of frogs. *Molecular Ecology Resources* **16**, 686–693. doi:10.1111/1755-0998.12492

Minh BQ, Schmidt HA, Chernomor O, Schrempf D, Woodhams MD, von Haeseler A, Lanfear R (2020) IQ-TREE 2: new models and efficient methods for phylogenetic inference in the genomic era. *Molecular Biology and Evolution* **37**, 1530–1534. doi:10.1093/molbev/msaa015

Naylor GJP, Caira JN, Jensen K, Rosana KAM, Straube N, Lakner C (2012) Elasmobranch phylogeny: a mitochondrial estimate based on 595 species. In 'Biology of Sharks and Their Relatives', 2nd edn. (Eds JC Carrier, JA Musick, MR Heithaus) pp. 31–56. (CRC Press, Taylor & Francis Group: Boca Raton, FL, USA) doi:10.1080/17451000.2012.745005

Olson PD, Littlewood DT, Bray RA, Mariaux J (2001) Interrelationships and evolution of the tapeworms (Platyhelminthes: Cestoda). *Molecular Phylogenetics and Evolution* **19**, 443–467. doi:10.1006/mpev.2001.0930

Pleijel F, Jondelius U, Norlinder E, Nygren A, Oxelman B, Schander C, Sundberg P, Thollesson M (2008) Phylogenies without roots? A plea for the use of vouchers in molecular phylogenetic studies. *Molecular Phylogenetics and Evolution* **48**, 369–371. doi:10.1016/j.ympev.2008.03.024

Reyda FB, Healy CJ, Haslach AR, Ruhnke TR, Aprill TL, Bergman MP, Daigler AL, Dedrick EA, Delgado I, Forti KS, Herzog KS, Russell RS, Willsey DD (2016) A new genus of rhinebothriidean cestodes from batoid elasmobranchs, with the description of five new species and two new combinations. *Folia Parasitologica* **63**, 038. doi:10.14411/fp.2016.038

Ruhnke TR, Caira JN, Cox A (2015) The cestode order Rhinebothriidea no longer family-less: a molecular phylogenetic investigation with erection of two new families and description of eight new species of *Anthocephalum*. *Zootaxa* **3904**, 51–81. doi:10.11646/zootaxa.3904.1.3

Ruhnke TR, Pommelle CP, Aguilar D, Hudson H, Reyda FB (2022) Two new species of *Stillabothrium* (Cestoda: Rhinebothriidea) from stingrays from northern Australia and one new combination. *Journal of Parasitology* **108**, 166–179. doi:10.1645/21-94

Schaeffner BC (2016) Review of the genus *Shirleyrhynchus* Beveridge & Campbell, 1988 (Trypanorhyncha: Shirleyrhynchidae), with the resurrection of *S. butlerae* Beveridge & Campbell, 1988 and the description of *S. panamensis* n. sp. *Systematic Parasitology* **93**, 413–430. doi:10.1007/s11230-016-9641-0

Tkach VV, Littlewood DT, Olson PD, Kinsella JM, Swiderski Z (2003) Molecular phylogenetic analysis of the Microphalloidea Ward, 1901 (Trematoda: Digenea). *Systematic Parasitology* **56**, 1–15. doi:10.1023/A:1025546001611

Trevisan B, Primon JF, Marques FPL (2017) Systematics and diversification of *Anindobothrium* Marques, Brooks, & Lasso, 2001 (Eucestoda: Rhinebothriidea). *PLoS ONE* **12**, e0184632. doi:10.1371/journal.pone.0184632

Trevisan B, Alcantara DMC, Machado DJ, Marques FPL, Lahr DJG (2019) Genome skimming is a low-cost and robust strategy to assemble complete mitochondrial genomes from ethanol preserved specimens in biodiversity studies. *PeerJ* **7**, e7543. doi:10.7717/peerj.7543

Trevisan B, Jacob Machado D, Lahr DJG, Marques FPL (2021) Comparative characterization of mitogenomes from five orders of cestodes (Eucestoda: Tapeworms). *Frontiers in Genetics* **12**, 788871. doi:10.3389/fgene.2021.788871

Van der Auwera G, Chapelle S, De Wächter R (1994) Structure of the large ribosomal subunit RNA of *Phytophthora megasperma*, and phylogeny of the oomycetes. *FEBS Letters* **338**, 133–136. doi:10.1016/0014-5793(94)80350-1

Wojciechowska A (1991) Some tetraphyllidean and diphyllidean cestodes from Antarctic batoid fishes. *Acta Parasitologica Polonica* **36**, 69–74.

Data availability. The sequence data generated for this study are available in GenBank.

Conflicts of interest. The authors declare that they have no conflicts of interest.

Declaration of funding. This work is supported by funds from the US National Science Foundation (NSF) DEB numbers 0818696, 0818823, 1921404 and 1921411, and from the Fundação de Amparo à Pesquisa do Estado de São Paulo (FAPESP) awards numbers 2017/11063-4, 2018/03534-0 and 2019/01453-5. The funders had no role in study design, data collection and analysis, decision to publish or preparation of the manuscript.

Acknowledgements. We thank Jorge Pérez Schultheiss of the Museo Nacional de Historia Natural Chile for providing photographs of holotype specimens and Anna Phillips from the Smithsonian National Museum of Natural History for loaning holotype specimens. We are grateful to Xuanhao Sun from the Electron Microscopy Laboratory at the University of Connecticut (UConn) for assistance with scanning electron microscopy. Hannah Ralicki generated part of the sequence data used in the phylogenetic analysis. Host icons were modified from silhouettes created by Ignacio Contreras (CC BY 3.0 DEED) and Eloisa Pinheiro Giareta (CC BY 4.0 DEED) obtained in Phylopic (phylopic.org).

Author affiliations

[A]Department of Ecology and Evolutionary Biology, University of Connecticut, Unit 3043, 75 N. Eagleville Road, Storrs, CT 006269-3043, USA.

[B]Department of Zoology, Universidade de São Paulo, Rua do Matão, Travessa 14 número 101, São Paulo, SP, CEP 05508-090, Brazil.